

Synthesis of amidines by palladium-mediated CO₂ extrusion followed by insertion of carbodiimides: translating mechanistic studies to develop a one-pot method.

Yang Yang,^a Asif Noor,^a Allan J. Canty,^b Alireza Ariaafard,^b
Paul S. Donnelly*,^a and Richard A. J. O'Hair*^a

- a. School of Chemistry, Bio21 Institute of Molecular Science and Biotechnology, The University of Melbourne, Victoria 3010, Australia.
- b. School of Physical Sciences, University of Tasmania, Private Bag 75, Hobart, Tasmania 7001, Australia.

* Phone: +613 8344-2452. Fax: +613 9347-5180. E-mail: rohair@unimelb.edu.au; pauld@unimelb.edu.au

Table of Contents

Discussion of overall thermochemistry for the ExIn transformation of carboxylic acids to amidines	S4
---	----

List of Tables

Table S1. : B3LYP-D3BJ/BS2 DFT calculated enthalpy and Gibbs free energy change (kcal/mol) for ExIn reactions for amidine preparation	S4
Table S2. M06/6-31G* DFT calculated enthalpy and Gibbs free energy change (kcal/mol)	S5
Table S3. Rate data for ion-molecule reactions of [(phen)Pd(O ₂ CAr)] ⁺ with ⁱ PrN=C=N ⁱ Pr.....	S7
Table S4. Crystal data and structure refinement for 5AII.HCl.H₂O	S26
Table S5. Crystal data and structure refinement for 5AIII.HCl.H₂O	S27

List of Figures

Figure S1 Conformers of amidines where X=H, OMe; R= ⁱ Pr, Cy, Ph. 5-1 is the <i>E-syn</i> isomer; 5-2 is the <i>E-anti</i> isomer; 5-3 is the <i>Z-syn</i> isomer; 5-4 is the <i>Z-anti</i> isomer	S4
--	----

Figure S2. Decarboxylation of [(phen)Pd(O ₂ CAr)] ⁺ under collision induced dissociation conditions: (a) [(phen)Pd(O ₂ CC ₆ H ₃ (2,6-OMe) ₂)] ⁺ , (b) [(phen)Pd(O ₂ CC ₆ H ₂ (2,4,6-OMe) ₃)] ⁺	S5
Figure S3. CID mass spectra at a normalized collision energy of 20 showing the fragmentation reactions of the products formed in the ion-molecule reaction between [(L)Pd(Ar)] ⁺ and ⁱ PrN=C=N ⁱ Pr.....	S6
Figure S4. Decarboxylation of [(Py) ₂ Pd(O ₂ CC ₆ H ₃ (2,6-OMe) ₂)] ⁺ under CID conditions	S6
Figure S5. Comparison between two isomers of 9d , Py <i>trans</i> to OMe and 9e , Py <i>cis</i> to OMe together with the complex 10e	S7
Figure S6. Pd(OAc) ₂ induced transformation of 2,6-dimethoxybenzoic acid to amidine 5AI monitored by ¹ H NMR spectroscopy (600Hz) in DMSO- <i>d</i> ₆	S8
Figure S7. Pd(TFA) ₂ induced transformation of 2,6-dimethoxybenzoic acid to amidine 5AII monitored by ¹ H NMR spectroscopy (600Hz) in DMSO- <i>d</i> ₆	S9
Figure S8. Pd(TFA) ₂ induced transformation of 2,6-dimethoxybenzoic acid to amidine 5AIII monitored by ¹ H NMR spectroscopy (600Hz) in DMSO- <i>d</i> ₆	S10
Figure S9. Pd(TFA) ₂ induced transformation of 2,4,6-trimethoxybenzoic acid to amidine 5BI monitored by ¹ H NMR spectroscopy	S11
Figure S10. Pd(TFA) ₂ induced transformation of 2,4,6-trimethoxybenzoic acid to amidine 5BII monitored by ¹ H NMR spectroscopy	S12
Figure S11. Pd(TFA) ₂ induced transformation of 2,4,6-trimethoxybenzoic acid to amidine 5BIII monitored by ¹ H NMR spectroscopy	S13
Figure S12. The ESI-HRMS spectrum (+ve, Thermo OrbiTrap MS) showing the isotope distribution patterns of the protonated amidine 5AI from ¹ H NMR monitoring experiment.....	S14
Figure S13. The ESI-HRMS spectrum (+ve, Thermo OrbiTrap MS) showing the isotope distribution patterns of the protonated amidine 5AII from ¹ H NMR monitoring experiment.....	S14
Figure S14. The ESI-HRMS spectrum (+ve, Thermo OrbiTrap MS) showing the isotope distribution patterns of the protonated amidine 5AIII from ¹ H NMR monitoring experiment.....	S15
Figure S15. The ESI-HRMS spectrum (+ve, Thermo OrbiTrap MS) showing the isotope distribution patterns of the protonated amidine 5BI from ¹ H NMR monitoring experiment.....	S15
Figure S16. The ESI-HRMS spectrum (+ve, Thermo OrbiTrap MS) showing the isotope distribution patterns of the protonated amidine 5BII from ¹ H NMR monitoring experiment	S16
Figure S17. The ESI-HRMS spectrum (+ve, Thermo OrbiTrap MS) showing the isotope distribution patterns of the protonated amidine 5BIII from ¹ H NMR monitoring experiment.....	S16
Figure S18. NMR spectra of isolated amidine 5AI : (a) ¹ H NMR (400MHz, DMSO- <i>d</i> 6); (b) ¹³ C NMR (400MHz, DMSO- <i>d</i> 6).....	S17

Figure S19. NMR spectra of isolated amidine 5AII : (a) ^1H NMR (400MHz, DMSO- <i>d</i> 6); (b) ^{13}C NMR (400MHz, DMSO- <i>d</i> 6).....	S17
Figure S20. NMR spectra of isolated amidine 5AIII : (a) ^1H NMR (400MHz, DMSO- <i>d</i> 6); (b) ^{13}C NMR (400MHz, DMSO- <i>d</i> 6).....	S18
Figure S21. NMR spectra of isolated amidine 5BI : (a) ^1H NMR (400MHz, DMSO- <i>d</i> 6); (b) ^{13}C NMR (400MHz, DMSO- <i>d</i> 6).....	S18
Figure S22. NMR spectra of isolated amidine 5BII : (a) ^1H NMR (400MHz, DMSO- <i>d</i> 6); (b) ^{13}C NMR (400MHz, DMSO- <i>d</i> 6).....	S19
Figure S23. NMR spectra of isolated amidine 5BIII : (a) ^1H NMR (400MHz, DMSO- <i>d</i> 6); (b) ^{13}C NMR (400MHz, DMSO- <i>d</i> 6).....	S19
X-ray Crystallography	S21
Figure S24. Mercury diagrams (capped stick) for the intermolecular hydrogen bonded arrangement of 5AII	S22
Figure S25. Mercury diagrams (capped stick) for the intermolecular hydrogen bonded arrangement of 5AII	S24
Structures and energies for all DFT calculated structures	S28
References	S33

Discussion of overall thermochemistry for the ExIn transformation of carboxylic acids to amidines.

DFT calculations were used to evaluate the enthalpy and Gibbs free energy (298K, gas phase) change associated with eq. 1 ($Y = NR$) for representative carboxylates and carbodiimides due to a dearth of literature on the heats of formation of amidines.³⁶ The M06/6-31G* method and level of theory was used as it closely matched the computationally more expensive G2 method for the model reaction shown in eq. S1 (B3LYP-D3BJ/BS2: $\Delta_rG = -24.7$ kcal/mol; $\Delta_rH = -26.3$ kcal/mol, M06/6-31G*: $\Delta_rG = -26.5$ kcal/mol; $\Delta_rH = -28.1$ kcal/mol versus G2: $\Delta_rG = -26.4$ kcal/mol; $\Delta_rH = -28.0$ kcal/mol). The energies associated with the aromatic systems shown in Scheme 2 were then examined. We note that the product amidines can exist as 4 different isomers (Figure S1) but **5-1** is the most stable (Table S2). DFT calculations (Table S1) indicate that ExIn reactions for amidine preparation (eq. 1, $X = NR$) are considerably exothermic for all the systems shown in Scheme 2.

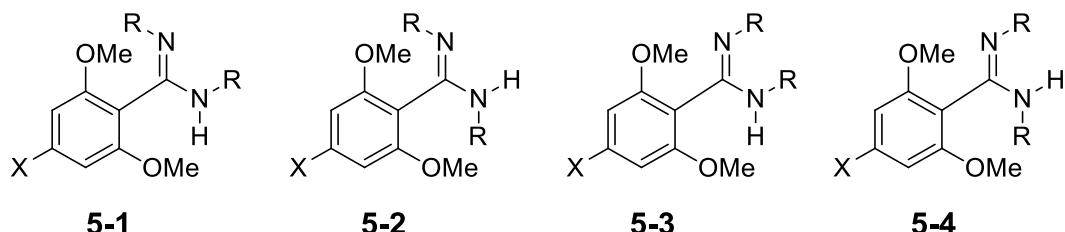


Figure S1: Conformers of amidines where $X=H, OMe$; $R=iPr, ^cHex, Ph$. **5-1** is the *E*-*syn* isomer; **5-2** is the *E*-*anti* isomer; **5-3** is the *Z*-*syn* isomer; **5-4** is the *Z*-*anti* isomer.³⁷

Table S1: B3LYP-D3BJ/BS2 DFT calculated enthalpy and Gibbs free energy change (kcal/mol) for ExIn reactions for amidine preparation (eq. 1, $Y = NR$).

Ar =	R =	Δ_rH	Δ_rG
2,6-(MeO) ₂ C ₆ H ₃	<i>i</i> Pr	-29.9	-24.8
2,6-(MeO) ₂ C ₆ H ₃	^c Hex	-30.4	-27.2
2,6-(MeO) ₂ C ₆ H ₃	Ph	-31.3	-26.5
2,4,6-(MeO) ₃ C ₆ H ₂	<i>i</i> Pr	-30.4	-26.1
2,4,6-(MeO) ₃ C ₆ H ₂	^c Hex	-31.1	-28.2
2,4,6-(MeO) ₃ C ₆ H ₂	Ph	-32.6	-29.2

Table S2: M06/6-31G* DFT calculated relative enthalpies and Gibbs free energies (kcal/mol) for the conformers of amidines. **5-1** is the *E-syn* isomer; **5-2** is the *E-anti* isomer; **5-3** is the *Z-syn* isomer; **5-4** is the *Z-anti* isomer.

X =	R =	5-1		5-2		5-3		5-4	
		$\Delta_r H$	$\Delta_r G$						
H	Me	0.0	0.0	1.6	0.8	7.6	7.6	3.7	3.5
H	<i>i</i> Pr	0.0	0.0	1.7	0.0	7.8	7.5	5.0	4.9
H	^c Hex	0.0	0.0	0.2	1.6	6.4	5.3	2.9	1.8
H	Ph	0.0	0.0	0.9	2.2	7.8	8.4	4.1	5.6
MeO	Me	0.0	0.0	1.5	1.1	9.6	10.4	2.1	4.1
MeO	<i>i</i> Pr	0.0	0.0	1.8	1.0	10.9	10.4	8.2	7.3
MeO	^c Hex	0.0	0.0	0.5	2.2	7.1	7.6	3.4	4.1
MeO	Ph	0.0	0.0	0.9	0.7	11.2	11.6	4.0	4.1

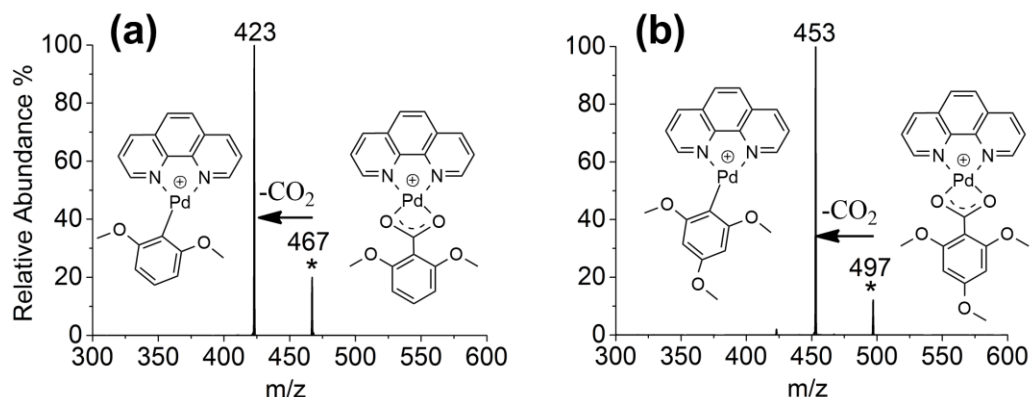


Figure S2. Decarboxylation of $[(\text{Phen})\text{Pd}(\text{O}_2\text{CCAr})]^+$ under collision induced dissociation conditions: (a) $[(\text{phen})\text{Pd}(\text{O}_2\text{CC}_6\text{H}_3(2,6\text{-OMe})_2)]^+$ ($m/z=467$), 100 ms, 13 eV, (b) $[(\text{phen})\text{Pd}(\text{O}_2\text{CC}_6\text{H}_2(2,4,6\text{-OMe})_3)]^+$ ($m/z=497$), 100 ms, 13 eV. The mass-selected precursor ions are denoted by a *.

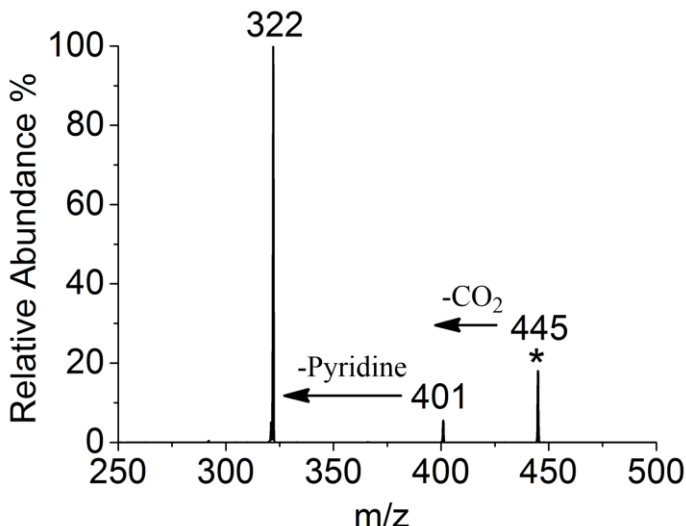


Figure S3. Decarboxylation of $[(\text{Py})_2\text{Pd}(\text{O}_2\text{CC}_6\text{H}_3(2,6\text{-OMe})_2)]^+$ ($m/z=445$) under CID conditions at a normalized collision energy of 14 eV. The mass-selected precursor ion is denoted by a *.

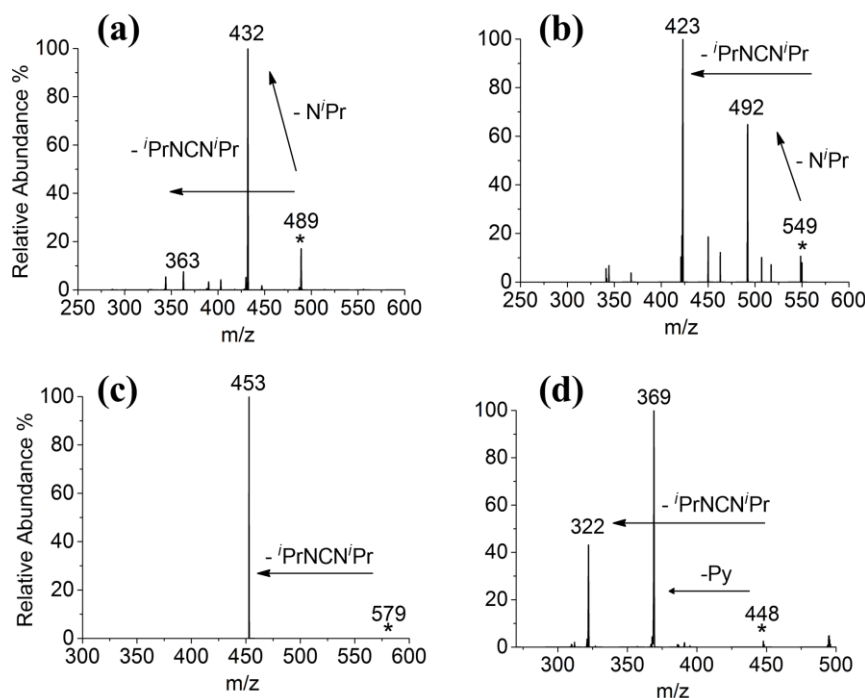


Figure S4. CID mass spectra at a normalized collision energy of 20 showing the fragmentation reactions of the products formed in the ion-molecule reaction between $[(\text{L})\text{Pd}(\text{Ar})]^+$ and $\text{iPrN}=\text{C}=\text{N}'\text{Pr}$: (a) L = phen, Ar = C_6H_5 ($m/z=489$), (b) L = phen, Ar = $\text{C}_6\text{H}_3(2,6\text{-OMe})_2$ ($m/z=549$), (c) L = phen, Ar = $\text{C}_6\text{H}_2(2,4,6\text{-OMe})_3$ ($m/z=579$), (d) L = py, Ar = $\text{C}_6\text{H}_3(2,6\text{-OMe})_2$ ($m/z=447$). iPr = isopropyl. The mass-selected precursor ion is denoted by a *.

Table S3. Ion-molecule kinetic data for reaction of $[(L)Pd(Ar)]^+$ and $iPrN=C=N^+iPr$:

L =	Ar =	$k_{expt}^{a,b}$	KADO^c	Φ^d
phen	C ₆ H ₅	1.416 x 10 ⁻⁹	1.179 x 10 ⁻⁹	120
py	C ₆ H ₃ (2,6-OMe) ₂	1.105 x 10 ⁻⁹	1.198 x 10 ⁻⁹	92

(a) Rates measured for these reactions were determined from triplicate experiments Mean \pm standard deviation (n=3). (b) In units of: cm³ molecules⁻¹ s⁻¹. (c) The k_{ADO} is the theoretical ion-molecule collision rate constant obtained from the average-dipole orientation (ADO) theory,¹ which is calculated using the Colrate program.² (d). Reaction efficiency, φ , = (k_{expt}/k_{ADO}) x 100.

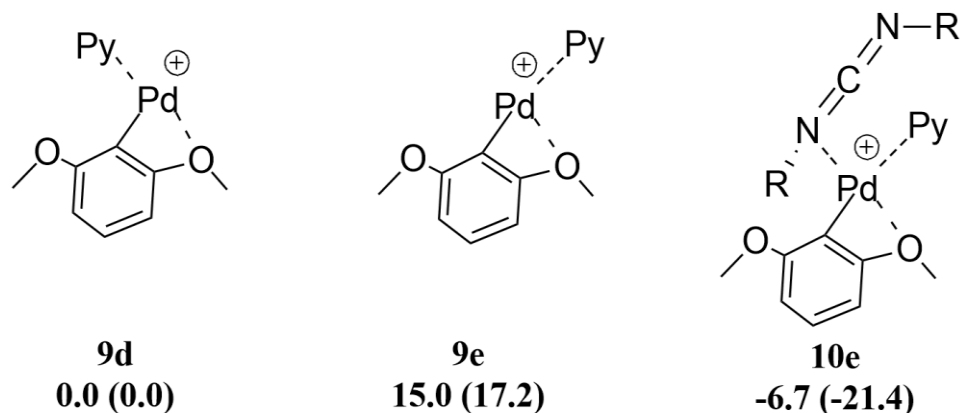


Figure S5. Comparison between two isomers of **9d**, Py *trans* to OMe and **9e**, Py *cis* to OMe together with the complex **10e**. The relative Gibbs and enthalpy energies (in parentheses) are given in kcal/mol and were calculated at the M06/LANL2DZ6-31G+(d) level of theory.

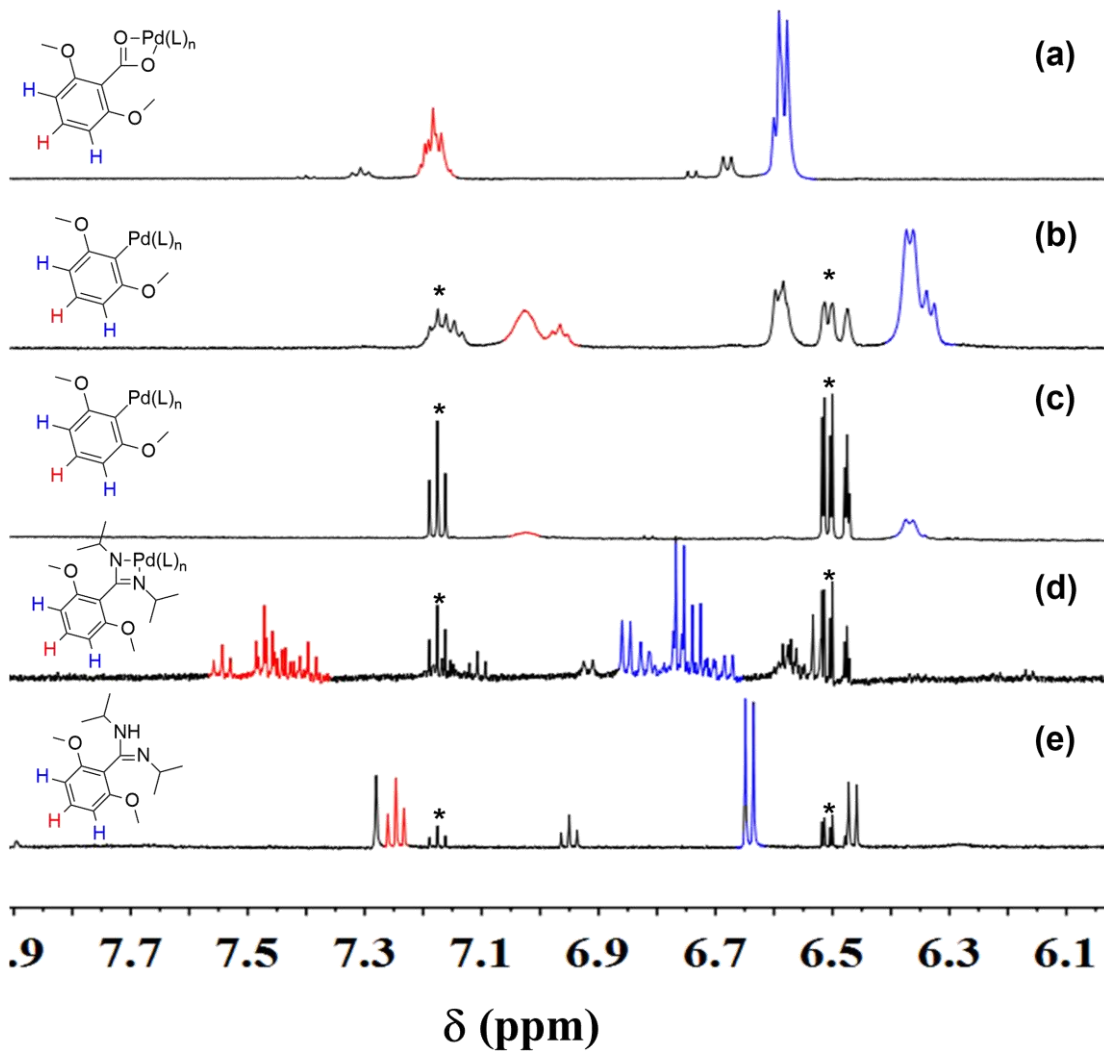


Figure S6. $\text{Pd}(\text{O}_2\text{CCH}_3)_2$ induced transformation of 2,6-dimethoxybenzoic acid to amidine **5AI** monitored by ^1H NMR spectroscopy (600Hz) in $\text{DMSO}-d_6$ (only the resonances due to the aromatic protons are shown): (a) 2,6-dimethoxybenzoic acid binding to the metal center (eq. 2); (b) decarboxylation for 4 hours (eq. 3); (c) showing heating for 24 hours to form the protodecarboxylation product completely (eq. 8); (d) insertion of $^i\text{PrN}=\text{C}=\text{N}^i\text{Pr}$ into the Pd-C bond (eq. 4) and (e) reaction of the palladium amidinate with NaBH_4 to release the free amidine (eq. 5). A * highlights peaks due to the product of protodecarboxylation, 1,3-dimethoxybenzene. Ligand 'L' is DMSO or acetate or both, $i\text{Pr}$ =isopropyl.

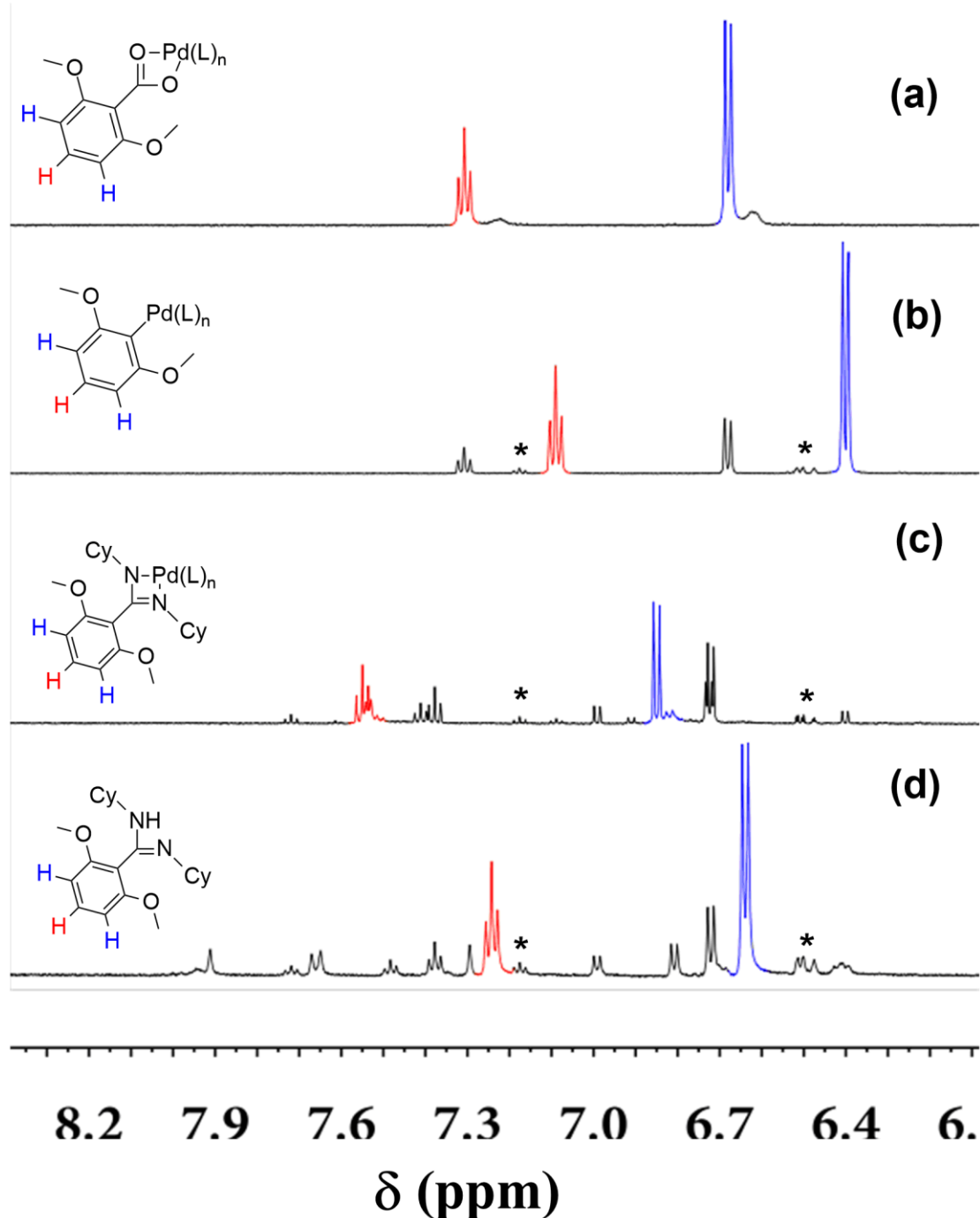


Figure S7. $\text{Pd}(\text{O}_2\text{CCF}_3)_2$ induced transformation of 2,6-dimethoxybenzoic acid to amidine **5AII** monitored by ^1H NMR spectroscopy (600Hz) in $\text{DMSO}-d_6$ (only the resonances due to the aromatic protons are shown): (a) 2,6-dimethoxybenzoic acid binding to the metal center (eq. 2); (b) decarboxylation for 6 hours (eq. 3); (c) insertion of $^6\text{HeN}=\text{C}=\text{N}^6\text{He}$ into the Pd-C bond (eq. 4) and (d) reaction of the palladium amidinate with NaBH_4 to release the free amidine (eq. 5). A * highlights peaks due to the product of protodecarboxylation, 1,3-dimethoxybenzene. Ligand 'L' is either DMSO or trifluoroacetate or both, $^6\text{He}=\text{cyclohexyl}$.

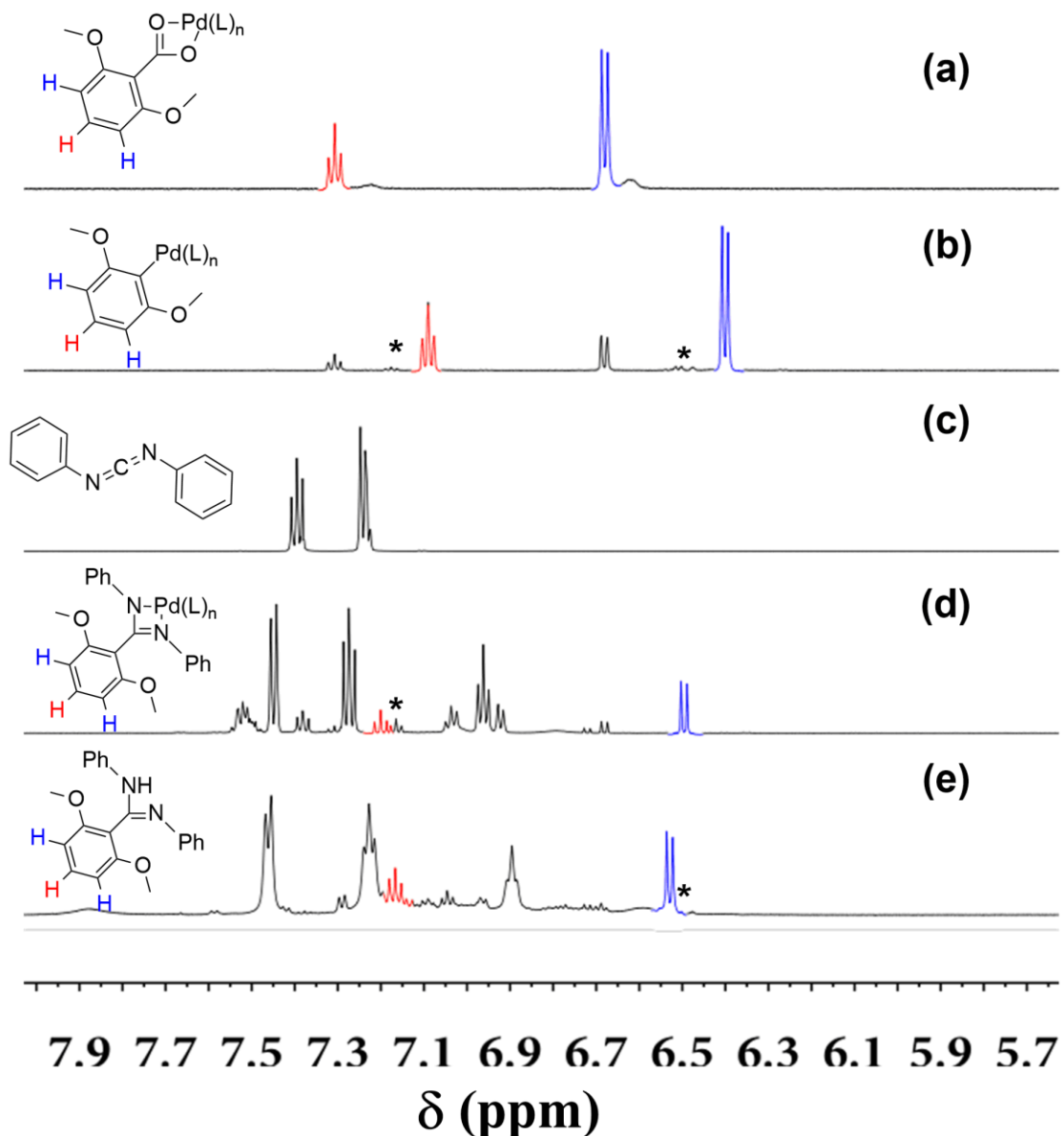


Figure S8. $\text{Pd}(\text{O}_2\text{CCF}_3)_2$ induced transformation of 2,6-dimethoxybenzoic acid to amidine **5AIII** monitored by ^1H NMR spectroscopy (600Hz) in $\text{DMSO}-d_6$ (only the resonances due to the aromatic protons are shown): (a) 2,6-dimethoxybenzoic acid binding to the metal center (eq. 2); (b) decarboxylation for 6 hours (eq. 3); (c) showing the peaks of $\text{PhN}=\text{C}=\text{NPh}$ at aromatic range; (d) insertion of $\text{PhN}=\text{C}=\text{NPh}$ into the Pd-C bond (eq. 4) and (e) reaction of the palladium amidinate with NaBH_4 to release the free amidine (eq. 5). A * highlights peaks due to the product of protodecarboxylation, 1,3-dimethoxybenzene. Ligand 'L' is either DMSO or trifluoroacetate or both.

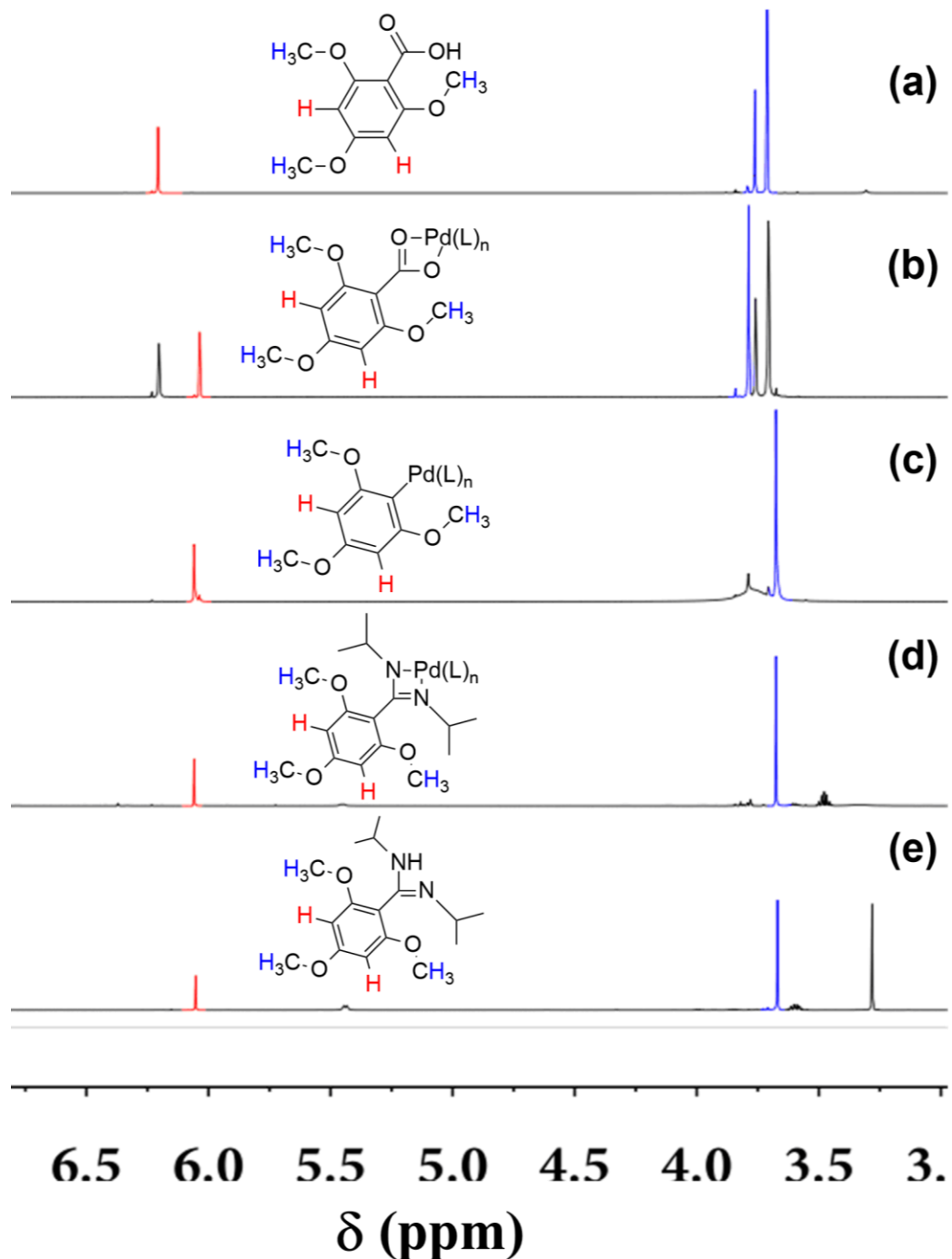


Figure S9. $\text{Pd(O}_2\text{CCF}_3)_2$ induced transformation of 2,4,6-trimethoxybenzoic acid to amidine **5BI** monitored by ^1H NMR spectroscopy (only the resonances due to the aromatic protons and methoxy protons are shown): (a) 2,4,6-trimethoxybenzoic acid; (b) 2,4,6-trimethoxybenzoic acid binding to the metal center (eq. 2); (c) decarboxylation for 6 hours (eq. 3); (d) insertion of $^i\text{PrN}=\text{C}=\text{N}^i\text{Pr}$ into the Pd-C bond (eq. 4) and (e) reaction of the palladium amidinate with NaBH_4 to release the free amidine (eq. 5). Ligand ‘L’ is either DMSO or trifluoroacetate or both, ^iPr =isopropyl.

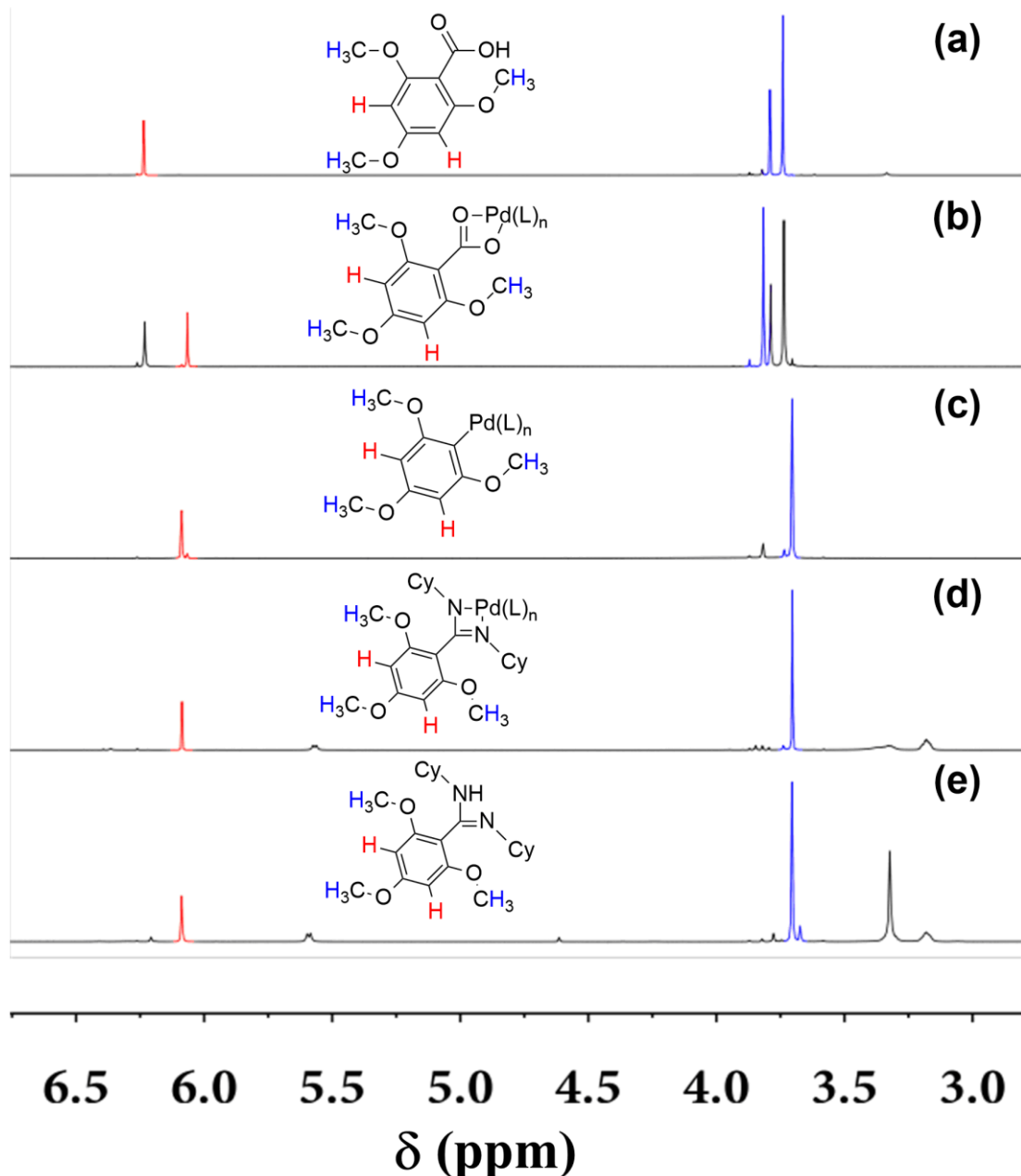


Figure S10. $\text{Pd}(\text{O}_2\text{CCF}_3)_2$ induced transformation of 2,4,6-trimethoxybenzoic acid to amidine **5BII** monitored by ^1H NMR spectroscopy (only the resonances due to the aromatic protons and methoxy protons are shown): (a) 2,4,6-trimethoxybenzoic acid; (b) 2,4,6-trimethoxybenzoic acid binding to the metal center (eq. 2); (c) decarboxylation for 6 hours (eq. 3); (d) insertion of $^c\text{HexN}=\text{C}=\text{N}^c\text{Hex}$ into the Pd-C bond (eq. 4) and (e) reaction of the palladium amidinate with NaBH_4 to release the free amidine (eq. 5). Ligand ‘L’ is either DMSO or trifluoroacetate or both, ^cHex =cyclohexyl.

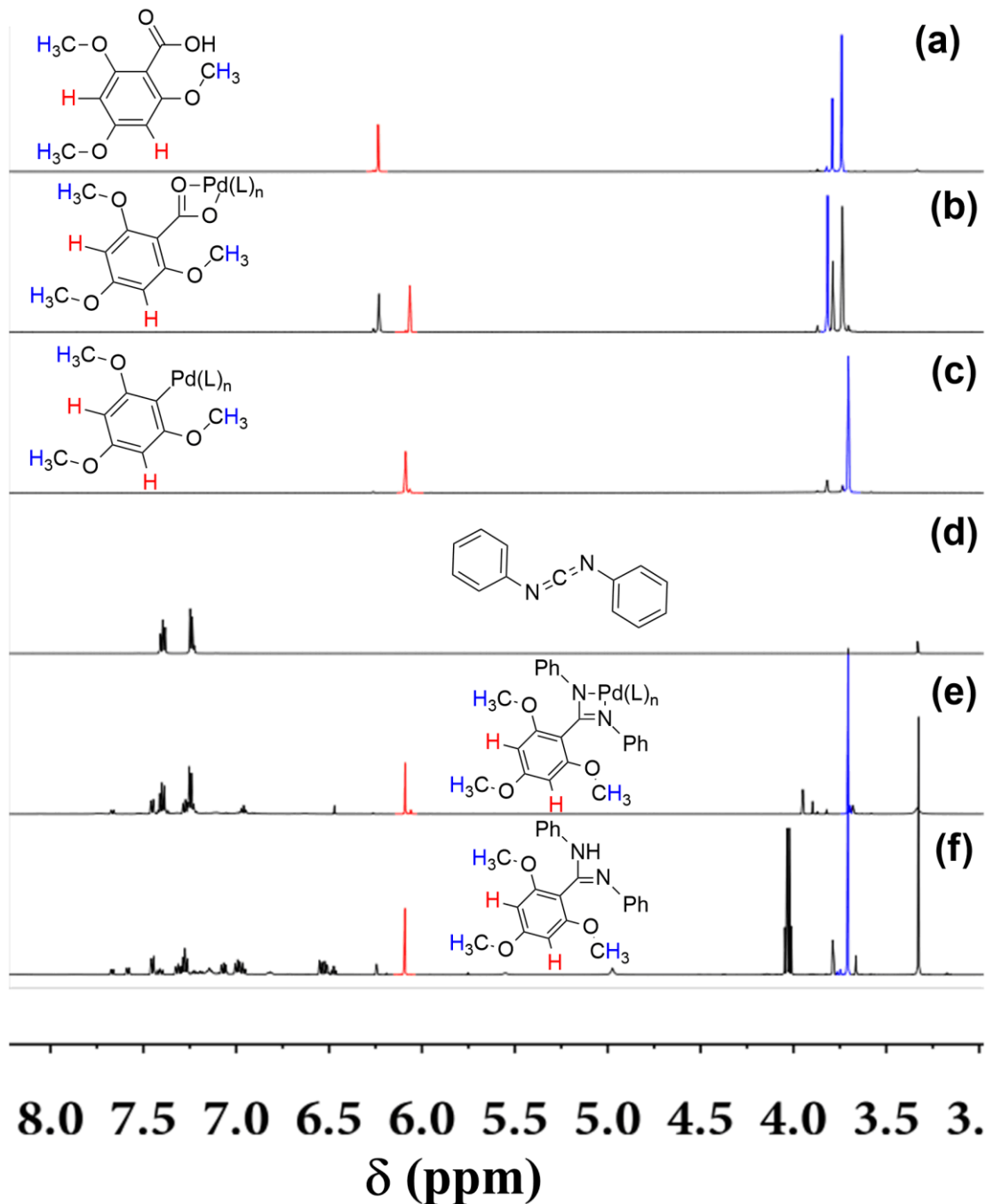


Figure S11. $\text{Pd}(\text{O}_2\text{CCF}_3)_2$ induced transformation of 2,4,6-trimethoxybenzoic acid to amidine **5BIII** monitored by ¹H NMR spectroscopy (only the resonances due to the aromatic protons and methoxy protons are shown): (a) 2,4,6-trimethoxybenzoic acid; (b) 2,4,6-trimethoxybenzoic acid binding to the metal center (eq. 2); (c) decarboxylation for 6 hours (eq. 3); (d) showing the peaks of $\text{PhN}=\text{C}=\text{NPh}$ at aromatic range (e) insertion of $\text{PhN}=\text{C}=\text{NPh}$ into the Pd-C bond (eq. 4) and (f) reaction of the palladium amidinate with NaBH_4 to release the free amidine (eq. 5). Ligand ‘L’ is either DMSO or trifluoroacetate or both.

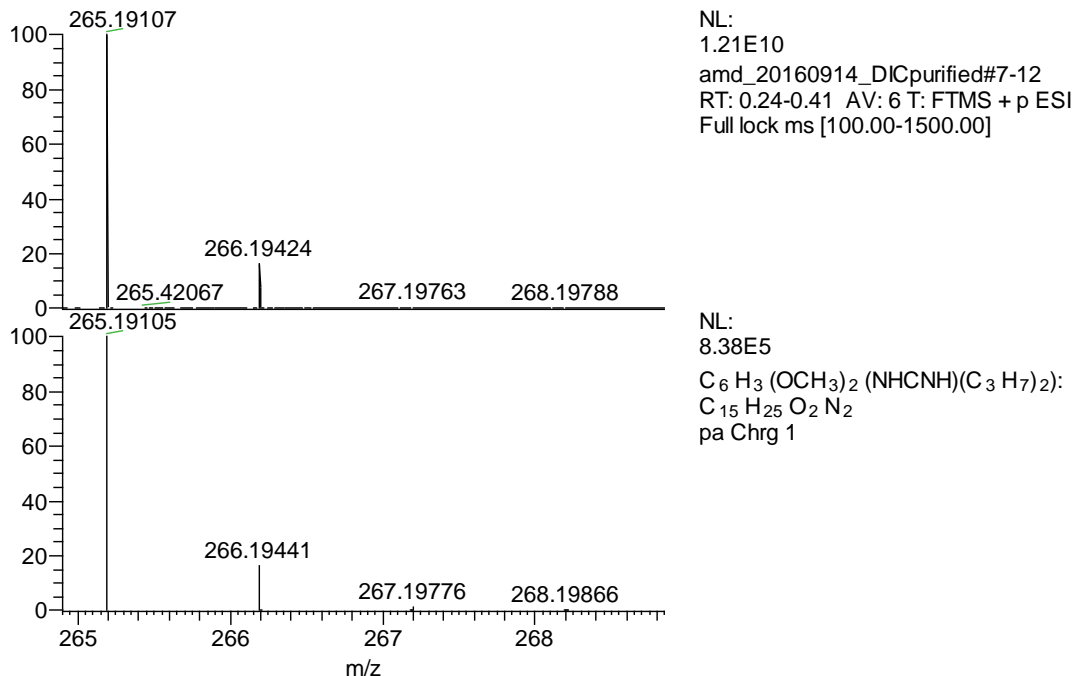


Figure S12. The ESI-HRMS spectrum (+ve, Thermo OrbiTrap MS) showing the isotope distribution patterns of the protonated amidine **5AI** formed in the ^1H NMR monitoring experiment (Figure S6). Observed (top) and calculated (bottom).

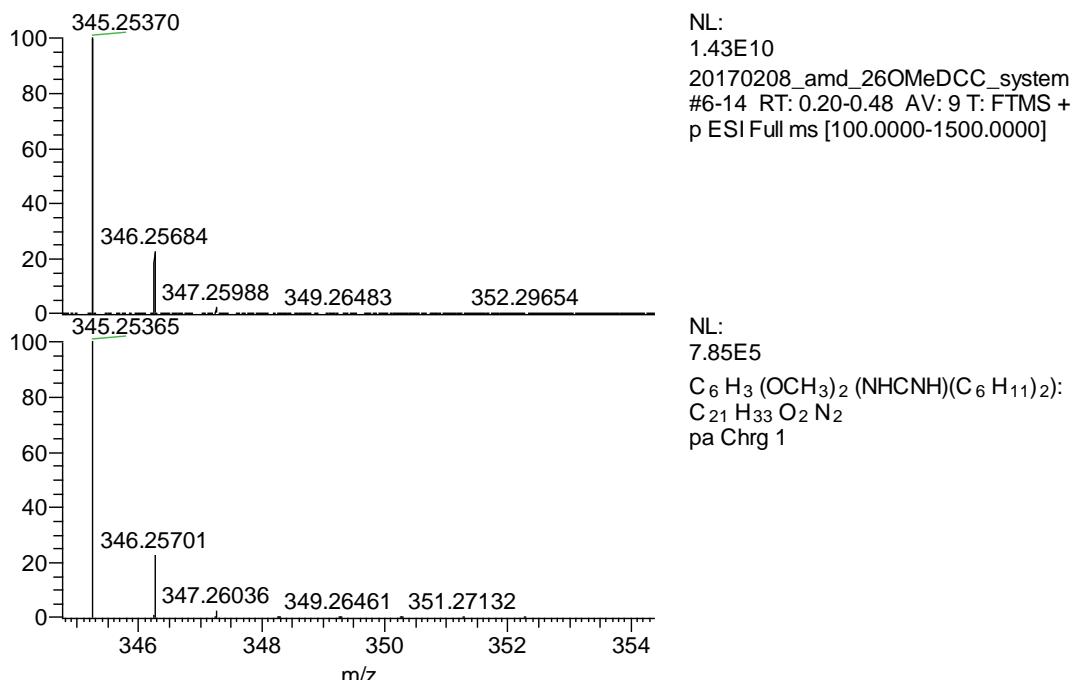


Figure S13. The ESI-HRMS spectrum (+ve, Thermo OrbiTrap MS) showing the isotope distribution patterns of the protonated amidine **5AII** formed in the ^1H NMR monitoring experiment (Figure S7). Observed (top) and calculated (bottom).

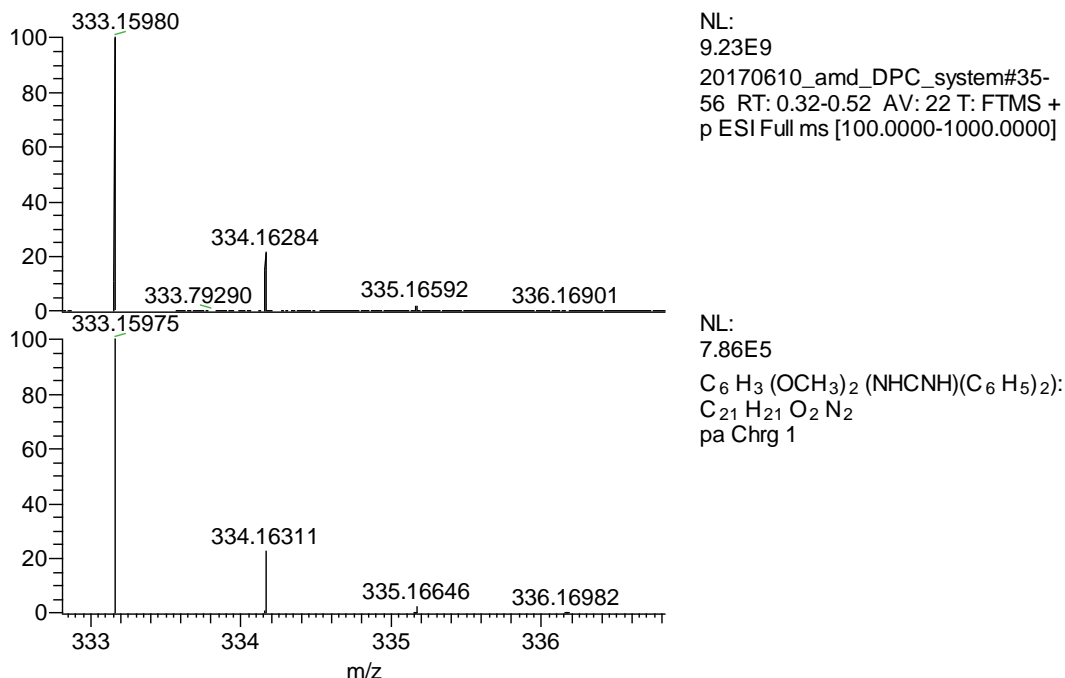


Figure S14. The ESI-HRMS spectrum (+ve, Thermo OrbiTrap MS) showing the isotope distribution patterns of the protonated amidine **5AIII** formed in the ^1H NMR monitoring experiment (Figure S8). Observed (top) and calculated (bottom).

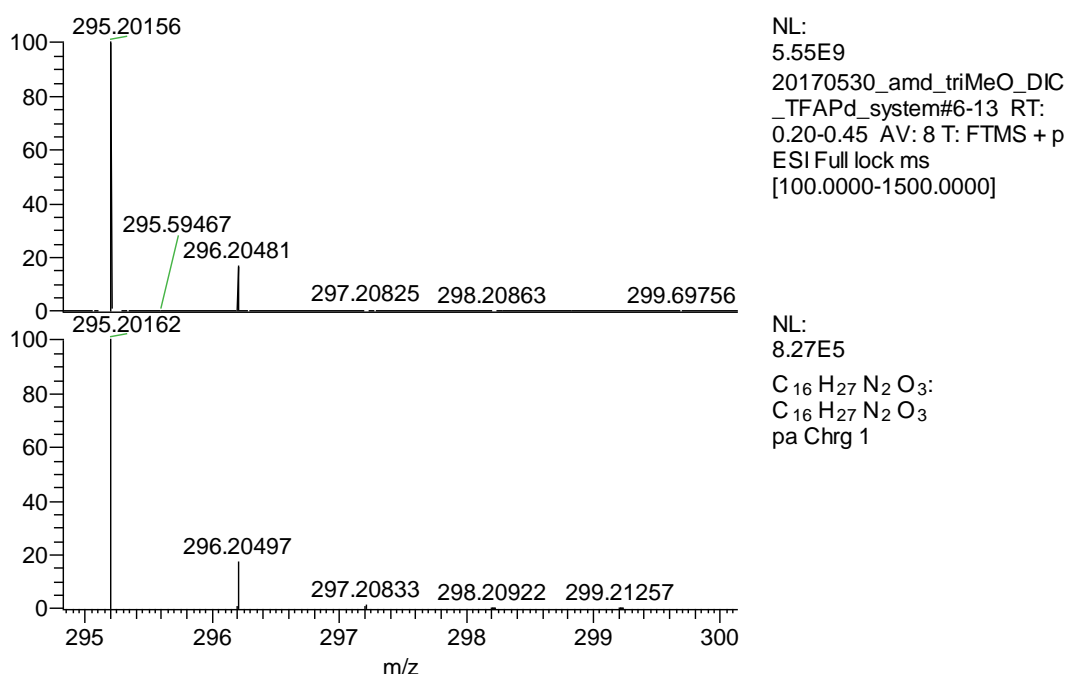


Figure S15. The ESI-HRMS spectrum (+ve, Thermo OrbiTrap MS) showing the isotope distribution patterns of the protonated amidine **5BI** formed in the ^1H NMR monitoring experiment (Figure S9). Observed (top) and calculated (bottom).

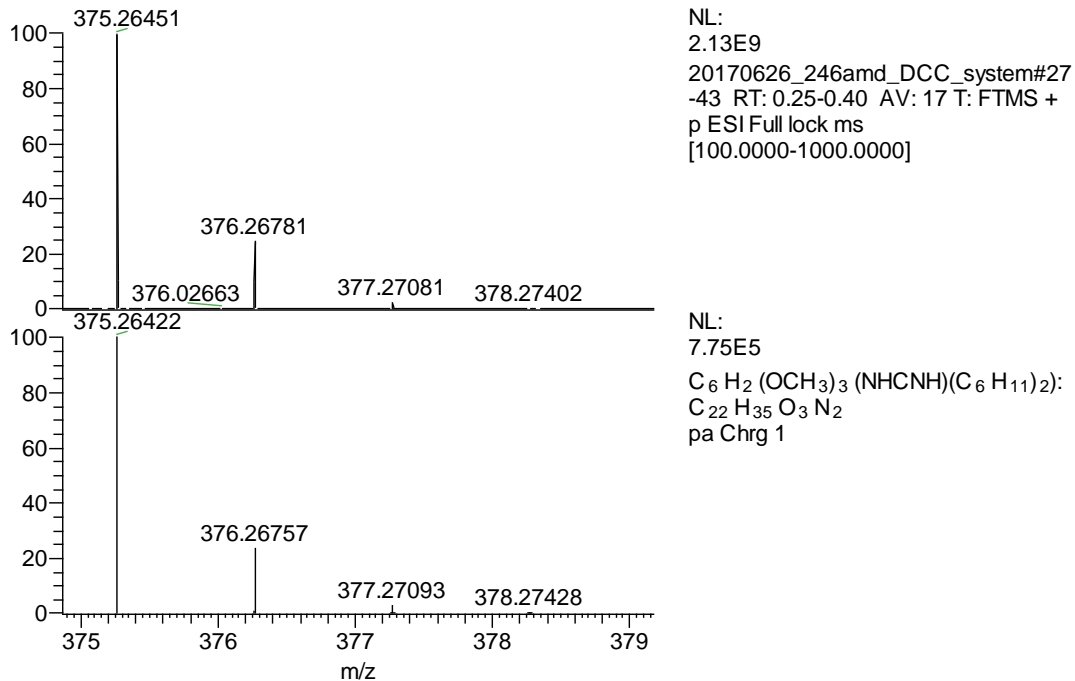


Figure S16. The ESI-HRMS spectrum (+ve, Thermo OrbiTrap MS) showing the isotope distribution patterns of the protonated amidine **5BII** formed in the ^1H NMR monitoring experiment (Figure S10). Observed (top) and calculated (bottom).

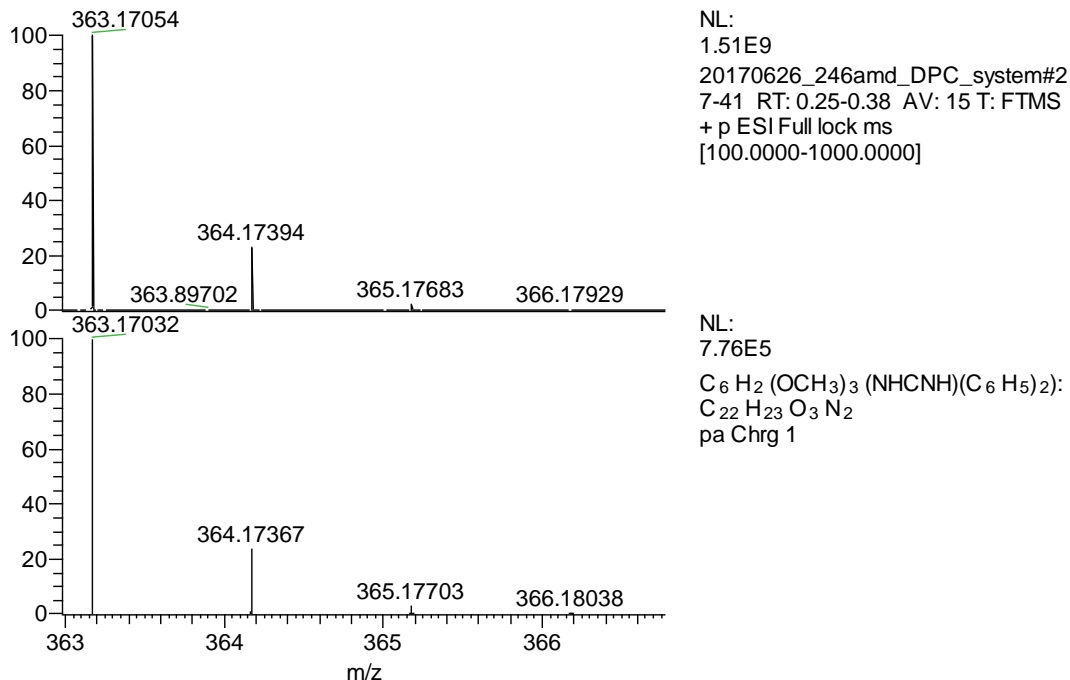


Figure S17. The ESI-HRMS spectrum (+ve, Thermo OrbiTrap MS) showing the isotope distribution patterns of the protonated amidine **5BIII** formed in the ^1H NMR monitoring experiment (Figure S11). Observed (top) and calculated (bottom).

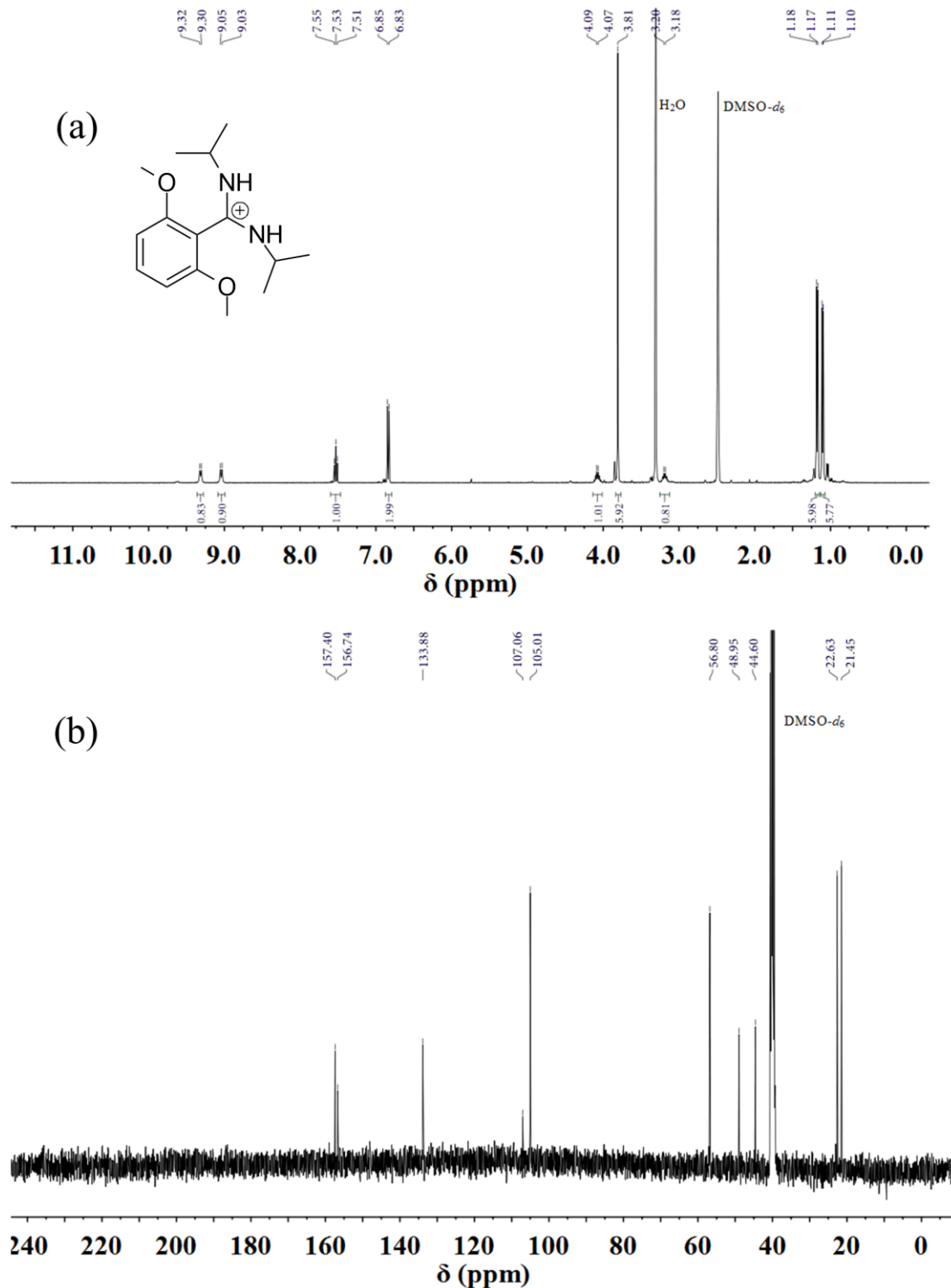


Figure S18. NMR spectra of isolated amidine **5AI**: (a) ^1H NMR (400MHz, DMSO-*d*₆); (b) ^{13}C NMR (400MHz, DMSO-*d*₆)

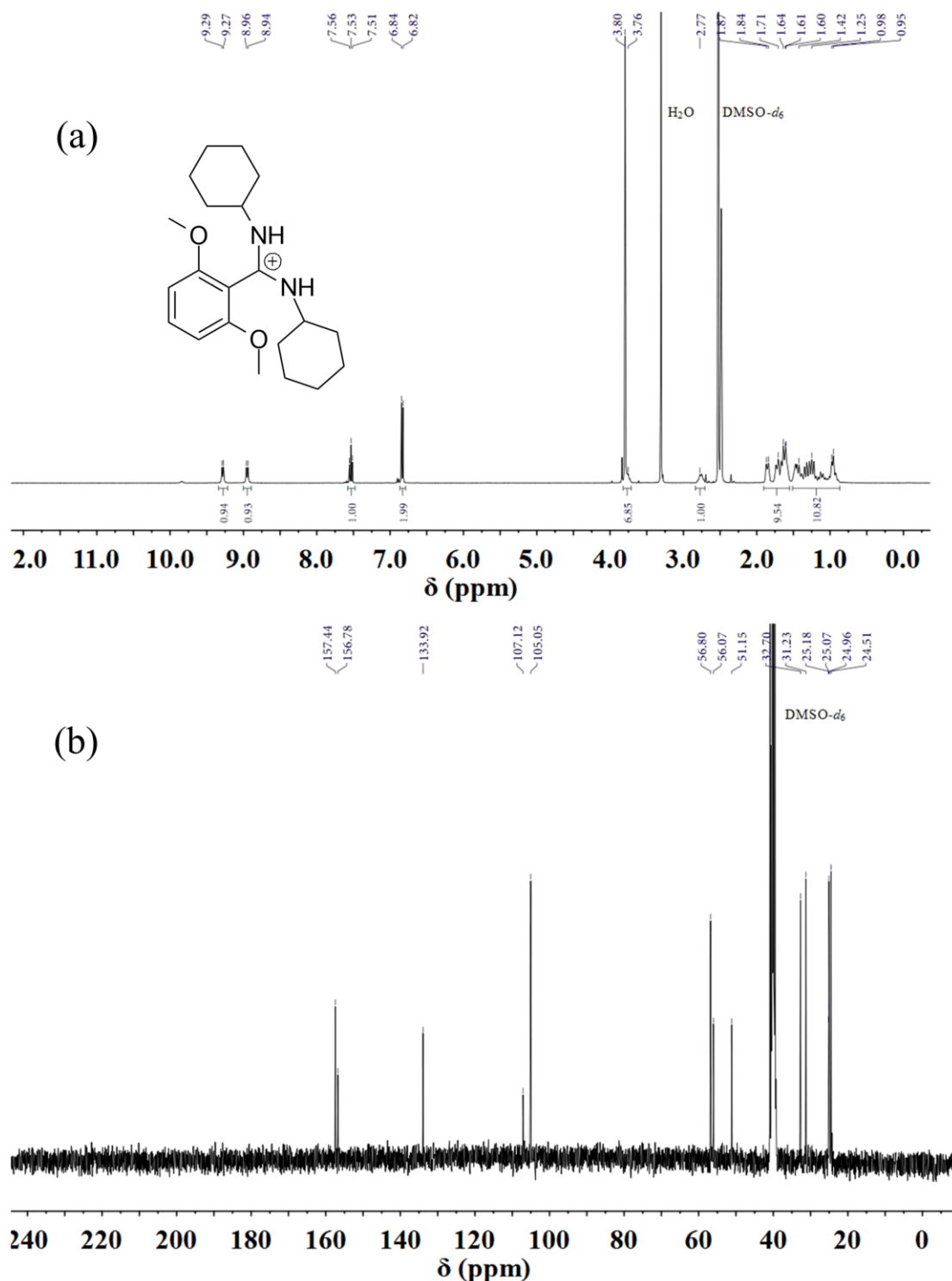


Figure S19. NMR spectra of isolated amidine **5AII**: (a) ^1H NMR (400MHz, $\text{DMSO}-d_6$); (b) ^{13}C NMR (400MHz, $\text{DMSO}-d_6$)

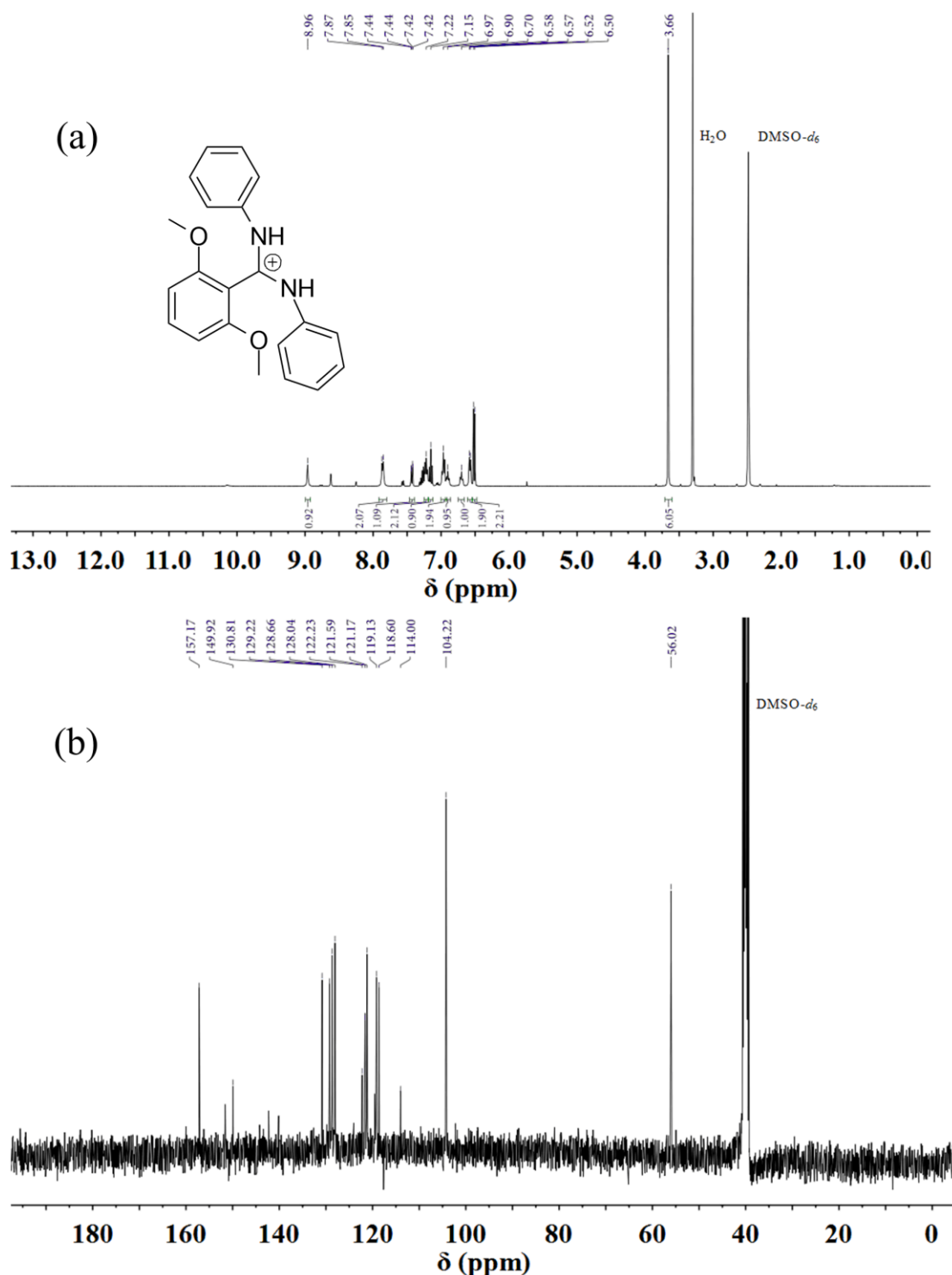


Figure S20. NMR spectra of isolated amidine 5AIII: (a) ¹H NMR (400MHz, DMSO-*d*₆); (b) ¹³C NMR (400MHz, DMSO-*d*₆)

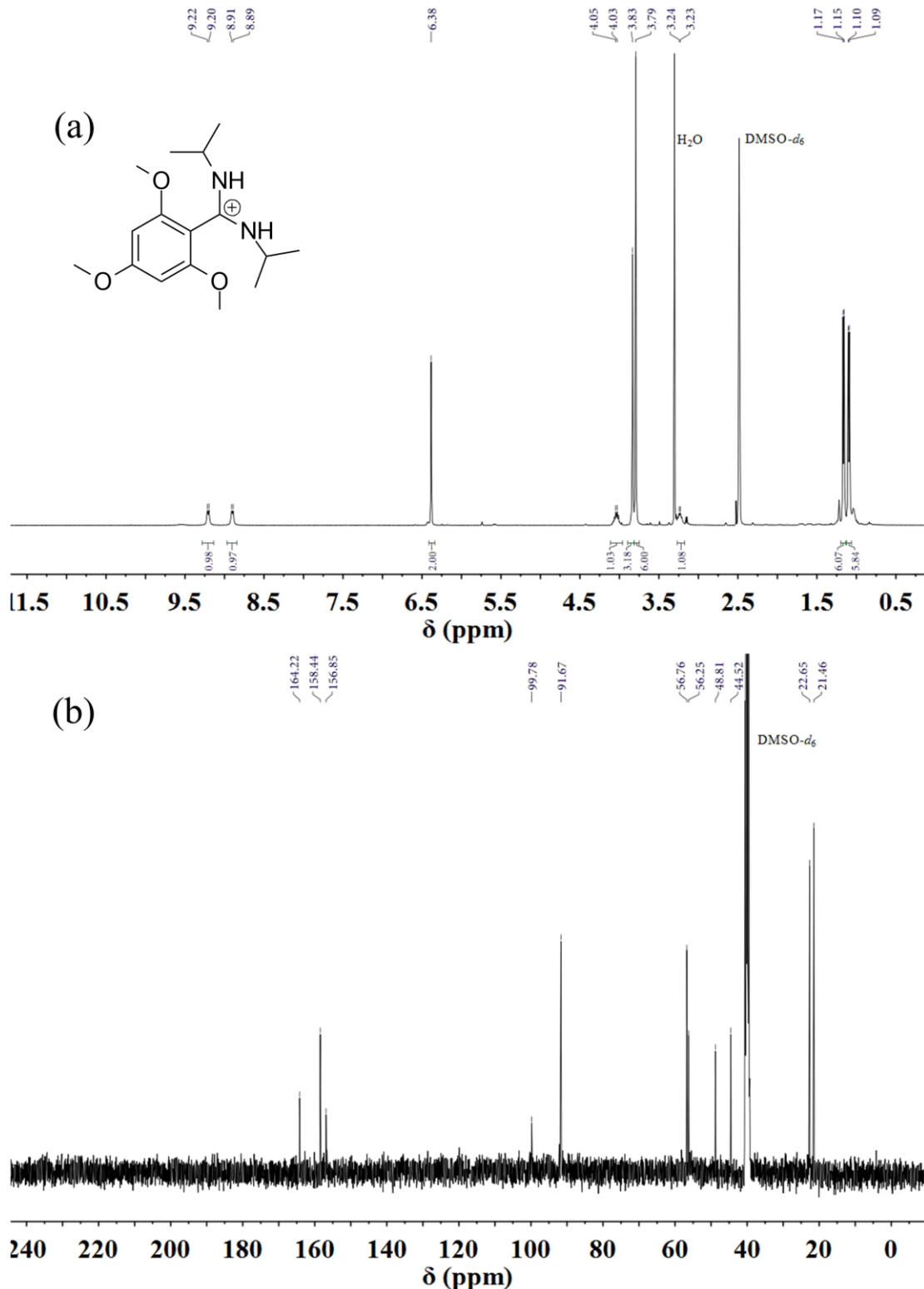


Figure S21. NMR spectra of isolated amidine **5BI**: (a) ¹H NMR (400MHz, DMSO-*d*₆); (b) ¹³C NMR (400MHz, DMSO-*d*₆)

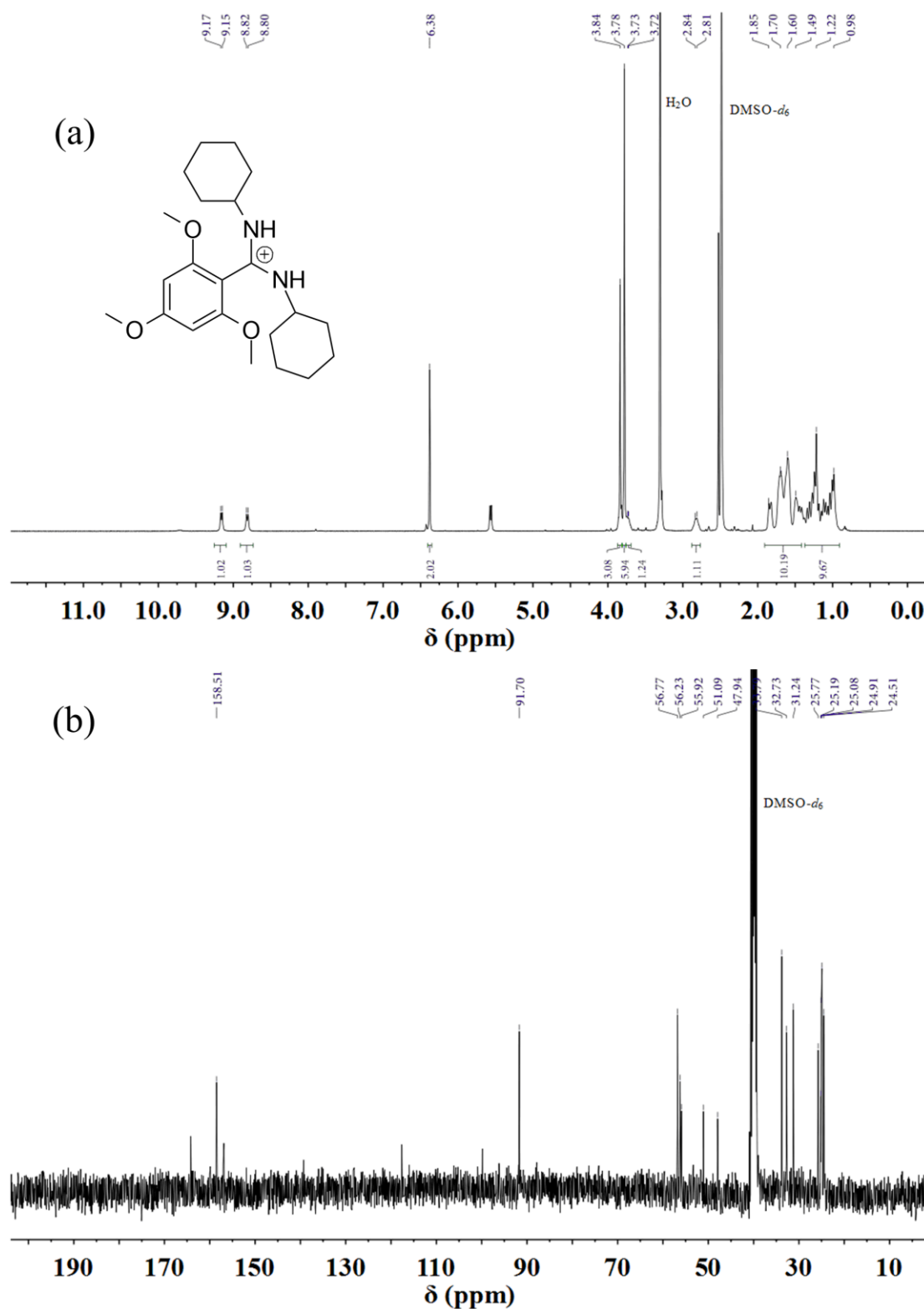


Figure S22. NMR spectra of isolated amidine **5BII**: (a) ^1H NMR (400MHz, DMSO- d_6); (b) ^{13}C NMR (400MHz, DMSO- d_6)

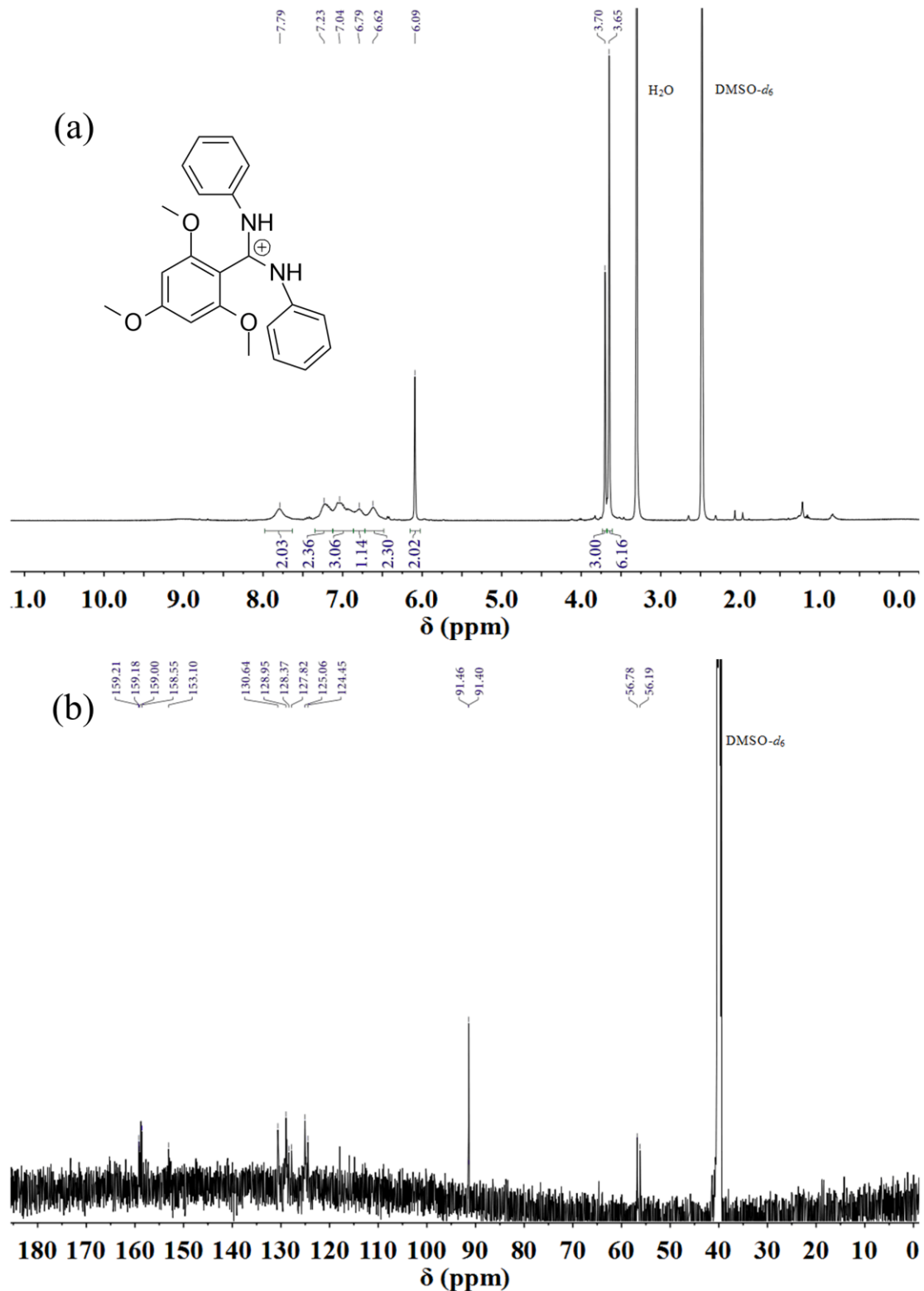


Figure S23. NMR spectra of isolated amidine **5BIII**: (a) ¹H NMR (400MHz, DMSO-*d*₆); (b) ¹³C NMR (600MHz, DMSO-*d*₆)

X-ray Crystallography

The molecular structures of the synthesized benzamidines **5AII** and **5AIII** as their hydrochloride salts were confirmed by X-ray crystallography. For both compounds single crystals suitable for X-ray diffraction were obtained by slow evaporation of compounds dissolved in a mixture of pentane and dichloromethane (1:1). Both benzamidine hydrochlorides crystallized with one benzamidinium cation, a chlorine atom and one water molecule in their asymmetric units but both structures show different intermolecular hydrogen bonded arrangements (Figures S24 and S25). A dimeric arrangement is found in **5AII.HCl.H₂O** supported by two water molecules at the centre and a bridging chlorine atom between the water molecule and **5AII.H⁺** due to strong hydrogen bonding through the Cl with O-H and N-H groups. In contrast, the hydrogen bonded arrangement in **5AIII** was different. Here two water molecules are bridged between a Cl atom and the **5AIII.H⁺** cation forming a hydrogen bonded zigzag chain in an extended supramolecular structure.

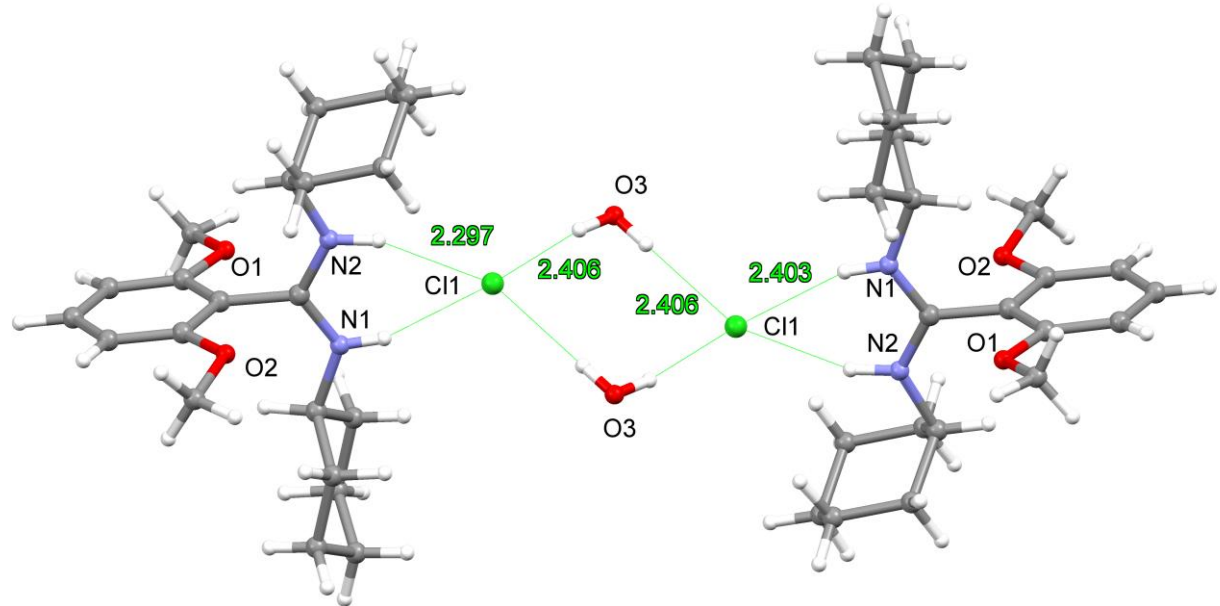


Figure S24. Mercury diagrams (capped stick) for the intermolecular hydrogen bonded arrangement of **5AII.HCl.H₂O**

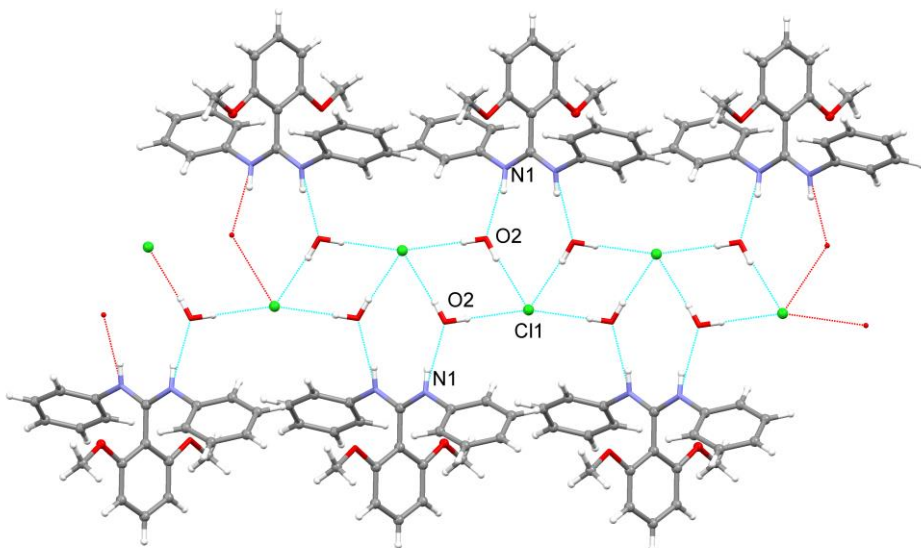


Figure S25. Mercury diagrams (capped stick) for the intermolecular hydrogen bonded arrangement of **5AII.HCl.H₂O**

Data Collection

X-ray data for amidines were collected at 130 K on an Agilent Technologies Dual source Supernova system using Mo and Cu K α radiation, and data were treated using CrysAlisPro^{*1} software. The structures were solved using SHELXT running within the WinGX^{*2} package program.

Data Refinement

X-Ray data refinement for 5AII·HCl·H₂O

The structure was solved by direct methods using SHELXT running within the WinGX^{*2} package. All non-hydrogen atoms were refined anisotropically. The structure was solved in the monoclinic space group $P2_1/n$ and refined to an R_I value of 4.8%. Full details are given in Table S4.

X-Ray data refinement for 5AIII.HCl.H₂O

The structure was solved by direct methods using SHELXT³ running within the WinGX⁴ package. All non-hydrogen atoms were refined anisotropically. The structure was solved in the monoclinic space group *I*2/*a* and refined to an *R*₁ value of 3.2%. Full details are given in Table S5.

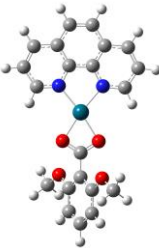
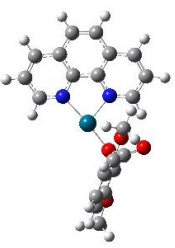
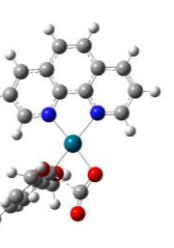
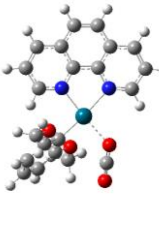
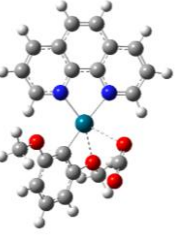
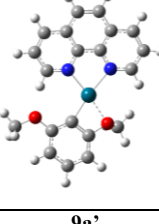
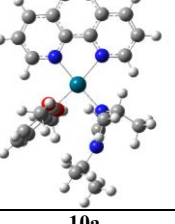
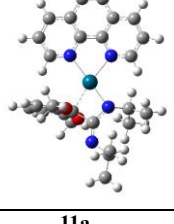
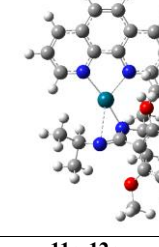
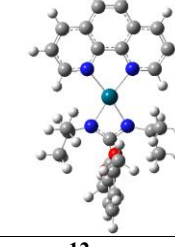
Table S4. Crystal data and structure refinement for **5AII.HCl.H₂O**

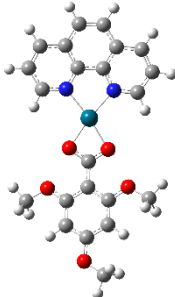
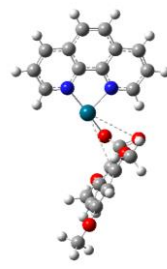
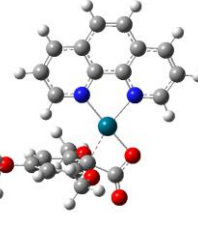
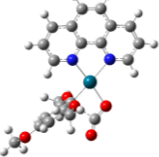
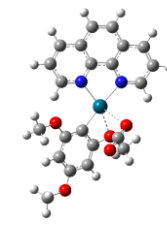
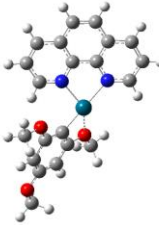
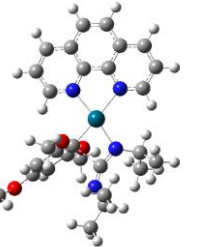
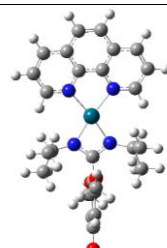
CCDC Number	1836504	
Identification code	5AII	
Empirical formula	C ₂₁ H ₃₅ C ₁ N ₂ O ₃	
Formula weight	398.96	
Temperature	130.00(10) K	
Wavelength	0.71073 Å	
Crystal system	Monoclinic	
Space group	P 21/n	
Unit cell dimensions	a = 10.1250(3) Å	α = 90°.
	b = 18.8393(5) Å	β = 108.937(4)°.
	c = 12.0041(4) Å	γ = 90°.
Volume	2165.83(12) Å ³	
Z	4	
Density (calculated)	1.224 Mg/m ³	
Absorption coefficient	0.199 mm ⁻¹	
F(000)	864	
Crystal size	0.617 x 0.400 x 0.261 mm ³	
Theta range for data collection	3.153 to 36.448°.	
Index ranges	-16<=h<=16, -31<=k<=20, -19<=l<=18	
Reflections collected	23758	
Independent reflections	10003 [R(int) = 0.0356]	
Completeness to theta = 25.242°	99.8 %	
Absorption correction	Gaussian	
Max. and min. transmission	0.944 and 0.898	
Refinement method	Full-matrix least-squares on F ²	
Data / restraints / parameters	10003 / 0 / 384	
Goodness-of-fit on F ²	1.032	
Final R indices [I>2sigma(I)]	R1 = 0.0480, wR2 = 0.1149	
R indices (all data)	R1 = 0.0715, wR2 = 0.1314	
Largest diff. peak and hole	0.471 and -0.326 e.Å ⁻³	

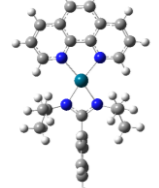
Table S5. Crystal data and structure refinement for **5AIII.HCl.H₂O**

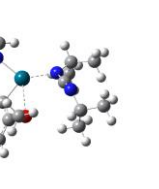
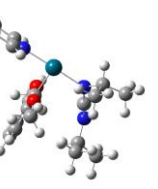
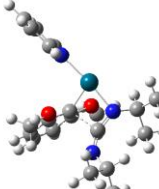
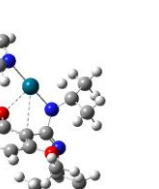
CCDC Number	1836505	
Identification code	5AIII	
Empirical formula	C ₂₁ H ₂₅ ClN ₂ O ₄	
Formula weight	404.88	
Temperature	130(10) K	
Wavelength	1.54184 Å	
Crystal system	Monoclinic	
Space group	I 2/a	
Unit cell dimensions	a = 9.6185(2) Å b = 16.7957(3) Å c = 12.7312(3) Å	α = 90°. β = 102.879(2)°. γ = 90°.
Volume	2004.98(7) Å ³	
Z	4	
Density (calculated)	1.341 Mg/m ³	
Absorption coefficient	1.936 mm ⁻¹	
F(000)	856	
Crystal size	0.391 x 0.275 x 0.141 mm ³	
Theta range for data collection	4.430 to 74.672°.	
Index ranges	-9<=h<=11, -17<=k<=20, -15<=l<=15	
Reflections collected	6781	
Independent reflections	2028 [R(int) = 0.0219]	
Completeness to theta = 67.684°	99.9 %	
Absorption correction	Semi-empirical from equivalents	
Max. and min. transmission	1.00000 and 0.59845	
Refinement method	Full-matrix least-squares on F ²	
Data / restraints / parameters	2028 / 0 / 179	
Goodness-of-fit on F ²	1.085	
Final R indices [I>2sigma(I)]	R1 = 0.0329, wR2 = 0.0867	
R indices (all data)	R1 = 0.0338, wR2 = 0.0878	
Extinction coefficient	n/a	
Largest diff. peak and hole	0.243 and -0.331 e.Å ⁻³	

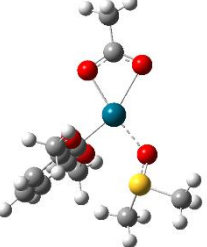
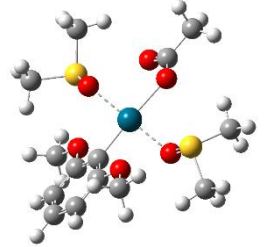
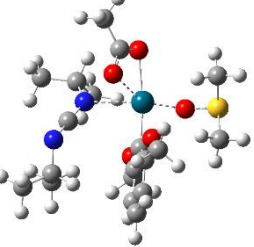
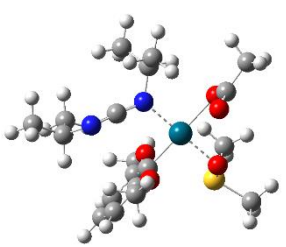
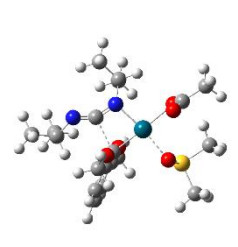
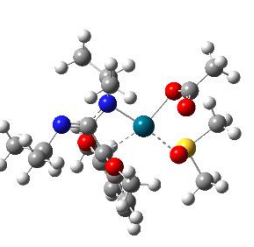
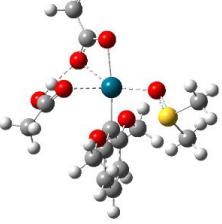
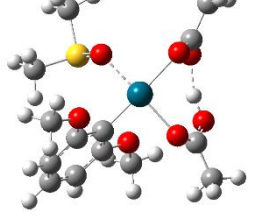
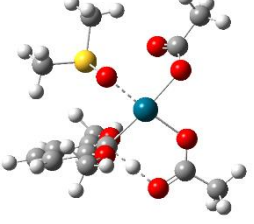
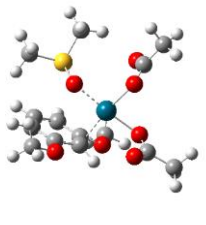
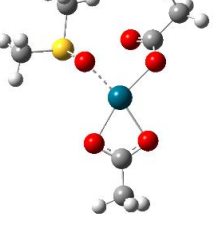
3D structures and energies for all M06/BS2 DFT calculated species (all energies are in Hartrees).

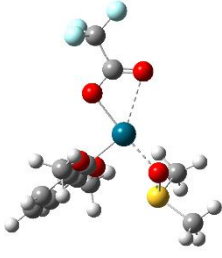
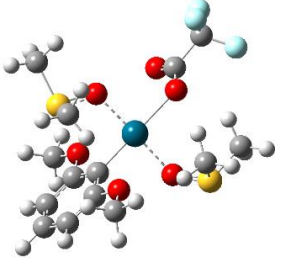
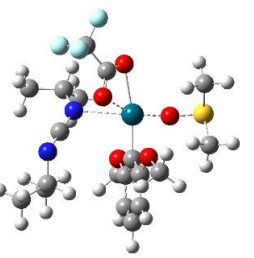
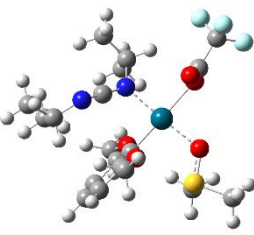
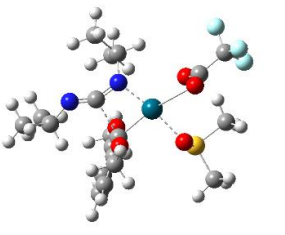
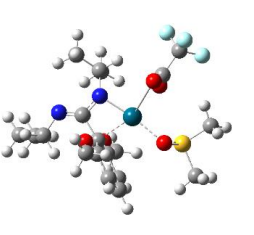
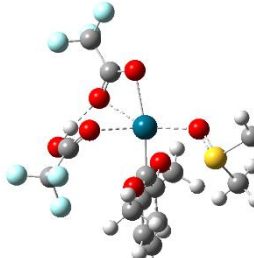
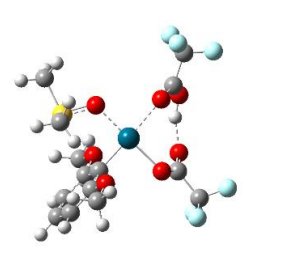
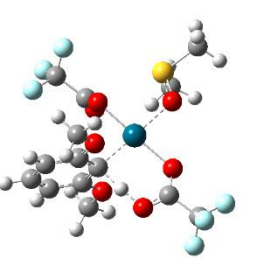
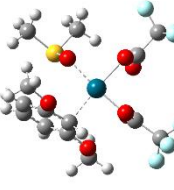
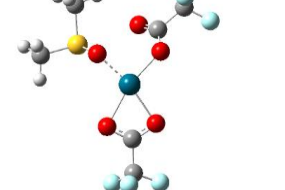
			
6a E= -1346.639114 H= -1346.269474 G= -1346.349352 SPE= -1349.269601	6a-7a E= -1346.579718 H= -1346.211523 G= -1346.288904 SPE= -1349.213386	7a E= -1346.636087 H= -1346.266935 G= -1346.346816 SPE= -1349.262731	TS7a-8a E= -1346.624478 H= -1346.257966 G= -1346.334835 SPE= -1349.250394
			
8a E= -1346.639918 H= -1346.271298 G= -1346.353862 SPE= -1349.26575	TS8a-9a' E= -1346.62691 H= -1346.259423 G= -1346.341619 SPE= -1349.254176	9a E= -1158.115745 H= -1157.764157 G= -1157.838387 SPE= -1160.569113	TS9a-9a' E= -1158.115709 H= -1157.765019 G= -1157.836656 SPE= -1160.569217
			
9a' E= -1158.126751 H= -1157.774798 G= -1157.847271 SPE= -1160.58278	10a E= -1542.553107 H= -1541.983305 G= -1542.082522 SPE= -1545.492054	10a-11a E= -1542.516789 H= -1541.948558 G= -1542.045130 SPE= -1545.452669	11a E= -1542.533567 H= -1541.962847 G= -1542.058715 SPE= -1545.465437
			
11a-12a E= -1542.51358 H= -1541.944725 G= -1542.039532 SPE= -1545.448129	12a E= -1542.565558 H= -1541.993332 G= -1542.089388 SPE= -1545.504509		

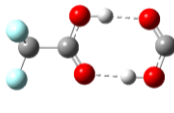
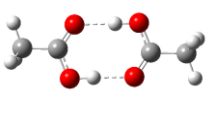
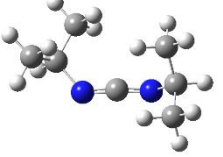
			
6b E= -1461.105495 H= -1460.699907 G= -1460.784847 SPE= -1463.850949	6b-7b E= -1461.044092 H= -1460.640564 G= -1460.72463 SPE= -1463.791962	7b E= -1461.106959 H= -1460.702185 G= -1460.786754 SPE= -1463.848803	7b-8b E= -1461.092951 H= -1460.68986 G= -1460.775123 SPE= -1463.835366
			
8b E= -1461.102706 H= -1460.697933 G= -1460.784673 SPE= -1463.843689	TS8b-9b' E= -1461.090084 H= -1460.68634 G= -1460.775844 SPE= -1463.833176	9b E= -1272.579673 H= -1272.192947 G= -1272.273207 SPE= -1275.147933	TS9b-9b' E= -1272.579055 H= -1272.193231 G= -1272.271537 SPE= -1275.147962
			
9b' E= -1272.589245 H= -1272.202339 G= -1272.27963 SPE= -1275.160388	10b E= -1657.015396 H= -1656.410053 G= -1656.515617 SPE= -1660.06961	TS10b-11b E= -1656.984455 H= -1656.380629 G= -1656.482625 SPE= -1660.036158	11b E= -1657.003698 H= -1656.397027 G= -1656.498857 SPE= -1660.050968
			
11b-12b E= -1656.976613 H= -1656.372487 G= -1656.472564 SPE= -1660.026188	12b E= -1657.029616 H= -1656.422386 G= -1656.526059 SPE= -1660.083677		

			
9c	10c	TS10c-11c	11c
E= -929.187882 H= -928.907834 G= -928.972577 SPE= -931.4087317	E= -1313.623934 H= -1313.124422 G= -1313.212486 SPE= -1316.331008	E= -1313.577454 H= -1313.081075 G= -1313.168116 SPE= -1316.281964	E= -1313.596218 H= -1313.096157 G= -1313.181927 SPE= -1316.299602
			
TS11c-12c	12c		
E= -1313.585049 H= -1313.087448 G= -1313.173472 SPE= -1316.289914	E= -1313.635058 H= -1313.134555 G= -1313.220857 SPE= -1316.343726		

			
9d	10d	TS10d-10d'	10d'
E= -834.990386 H= -834.726368 G= -834.789694 SPE= -837.0588468	E= -1219.408456 H= -1218.926401 G= -1219.016422 SPE= -1221.962058	E= -1219.391818 H= -1218.910316 G= -1218.998211 SPE= -1221.942368	E= -1219.422793 H= -1218.940014 G= -1219.02863 SPE= -1221.973846
			
TS10d'-11d	11d	TS11d-11d'	11d'
E= -1219.38338 H= -1218.902672 G= -1218.989355 SPE= -1221.930513	E= -1219.399996 H= -1218.917426 G= -1219.004511 SPE= -1221.943792	E= -1219.375711 H= -1218.897839 G= -1218.983271 SPE= -1221.924234	E= -1219.376306 H= -1218.896253 G= -1218.981978 SPE= -1221.925086
			
TS11d'-12d	12d		
E= -1219.374665 H= -1218.89359 G= -1218.979207 SPE= -1221.919806	E= -1219.42047 H= -1218.937268 G= -1219.027492 SPE= -1221.97158		

		
13a1 E = -1368.580509 H = -1368.269103 G = -1368.345382 SPE = -1370.846982630	13a2 E = -1921.659037 H = -1921.258399 G = -1921.349693 SPE = -1924.195395050	TS13a-14a E = -1752.954818 H = -1752.425937 G = -1752.528191 SPE = -1755.702346950
		
14a E = -1752.974198 H = -1752.443246 G = -1752.545146 SPE = -1755.725718240	TS14a-15a E = -1752.950554 H = -1752.421521 G = -1752.523478 SPE = -1755.700271980	15a E = -1752.982071 H = -1752.450895 G = -1752.552188 SPE = -1755.727585860
		
TS13a-16a E = -1597.547468 H = -1597.166233 G = -1597.252927 SPE = -1600.049815500	16a E = -1597.565397 H = -1597.184293 G = -1597.271939 SPE = -1600.072961960	TS16a-17a E = -1597.549975 H = -1597.168089 G = -1597.256653 SPE = -1600.050781170
		
17a E = -1597.563914 H = -1597.182074 G = -1597.273094 SPE = -1600.068971240	18a E = -1136.569155 H = -1136.366067 G = -1136.431849 SPE = -1138.540605970	

		
13b1 E = -1666.223517 H = -1665.931735 G = -1666.015463 SPE = -1668.699794	13b2 E = -2219.308614 H = -2218.928027 G = -2219.0262 SPE = -2222.057655	TS13b-14b E = -2050.602507 H = -2050.092194 G = -2050.195812 SPE = -2053.557664
		
14b E = -2050.628777 H = -2050.118724 G = -2050.228018 SPE = -2053.590696	TS14b-15b E = -2050.603067 H = -2050.094018 G = -2050.200544 SPE = -2053.56168	15b E = -2050.632954 H = -2050.122025 G = -2050.228165 SPE = -2053.5868
		
TS13b-16b E = -2192.831448 H = -2192.491284 G = -2192.58732 SPE = -2195.748819	16b E = -2192.850642 H = -2192.510262 G = -2192.612636 SPE = -2195.776215	TS16b-17b E = -2192.830835 H = -2192.495405 G = -2192.593724 SPE = -2195.755544
		
17b E = -2192.85925 H = -2192.517678 G = -2192.617609 SPE = -2195.783198	18b E = -1731.847602 H = -1731.685348 G = -1731.762189 SPE = -1734.238212	

			
(CF₃COOH)₂ E = -1053.2153 H = -1053.119511 G = -1053.178197 SPE = -1054.114081	(CH₃COOH)₂ E = -457.947255 H = -457.812168 G = -457.856 SPE = -458.428898430	DMSO E = -553.055231 H = -552.969371 G = -553.004256 SPE = -553.332269389	1,3-dimethoxy benzene E = -460.976633 H = -460.801079 G = -460.84928 SPE = -461.515425887
			
N,N'-diisopropyl carbodiimide E = -384.367711 H = -384.151883 G = -384.199959 SPE = -384.851308027			

References:

- (1) Su, T.; Bowers, M. T. Ion-polar molecule collisions. Effect of size on ion-polar molecule rate constants. Paramterization of the average-dipole-orientation theory. *Int. J. Mass Spectrom. Ion Phys.* **1973**, *12*, 347–356.
- (2) Lim, K. F. COLRATE. QCPE 643: Calculation of gas-kinetic collision rate coefficients. *QCPE Bull.* **1994**, *14*, 3.
- (3) CrysAlis PRO Software; Agilent Technologies: Yarnton, Oxfordshire, England, **2012**.
- (4) Farrugia, L. J. WinGX suite for small-molecule single-crystal crystallography, *J. Appl. Cryst.* **1999**, *32*, 837-838.